# Spike solutions in Gierer-Meinhardt model with a time dependent anomaly exponent

Yana Nec
Thompson Rivers University, 805 TRU Way, Kamloops, British Columbia, Canada,

*email: cranberryana@gmail.com*

## Abstract

Experimental evidence of complex dispersion regimes in natural systems, where the growth of the mean square displacement in time cannot be characterised by a single power, has been accruing for the past two decades. In such processes the exponent $\gamma(t)$ in $\langle r^2\rangle \sim t^{\gamma(t)}$ at times might be approximated by a piecewise constant function, or it can be a continuous function. Variable order differential equations are an emerging mathematical tool with a strong potential to model these systems. However, variable order differential equations are not tractable by the classic differential equations theory. This contribution illustrates how a classic method can be adapted to gain insight into a system of this type. Herein a variable order Gierer-Meinhardt model is posed, a generic reaction– diffusion system of a chemical origin. With a fixed order this system possesses a solution in the form of a constellation of arbitrarily situated localised pulses, when the components' diffusivity ratio is asymptotically small. The pattern was shown to exist subject to multiple step-like transitions between normal diffusion and sub-diffusion, as well as between distinct sub-diffusive regimes. The analytical approximation obtained permits qualitative analysis of the impact thereof. Numerical solution for typical cross-over scenarios revealed such features as earlier equilibration and non-monotonic excursions before attainment of equilibrium. The method is general and allows for an approximate numerical solution with any reasonably behaved $\gamma(t)$.

**Keywords:** fractional differential equations, matched asymptotic expansions, variable order differential equations, numerical estimates of memory integrals

## 1. Background

Beginning circa 1980 measurements of dispersion in various natural systems documented behaviour that could not be captured faithfully by a linear growth of the mean square displacement $\langle r^2\rangle \sim t$. In time such systems were termed anomalous. Spanning numerous scientific fields, the underpinning diffusive processes can be catalogued by basic transport properties, often including the Fickian diffusion as a special limit (Codling et al., 2008; Eliazar and Klafter, 2011). The sui generis nature of each anomalous process notwithstanding, wide sub-classes have been identified (Klages et al., 2008). The present contribution addresses a type of anomaly named sub-diffusion due to the sub-linear dispersion $\langle r^2\rangle \sim t^{\gamma}$ with $0<\gamma<1$. One way to obtain this kind of transport is to generalise the integer derivative in the diffusion equation to one of a fractional order (Metzler and Klafter, 2000). Mathematically an integer

order partial differential equation for the concentration of components $\mathbf{u}$ with a constant diffusion coefficient $\mathfrak{D}$ and source $\mathbf{f}(\mathbf{u})$

$$\mathbf{u}_t = \mathfrak{D}\Delta\mathbf{u} + \mathbf{f}(\mathbf{u}), \qquad \mathbf{r} \in \Omega, \quad t > 0, \tag{1a}$$

will become a fractional partial differential equation

$$\mathbf{u}_t^\gamma = \mathfrak{D}\Delta\mathbf{u} + \mathbf{f}(\mathbf{u}), \qquad \mathbf{r} \in \Omega, \quad t > 0. \tag{1b}$$

Over a certain range of time the dispersion $r = |\mathbf{r}|$ in the domain $\Omega$ will exhibit sub-diffusion with a mean square displacement that grows in time with the exponent $\gamma$. Within this framework the index $\gamma$ need not be constant, albeit traditionally it has been fixed.

Whilst the integer derivative operator is indisputably unique, multifarious fractional derivatives exist. For a constant $\gamma$ the most classic definition appears in Oldham and Spanier (1974), whereas more specialised operators can be found for instance in Elliot (1993) and Chen et al. (2010), as well as in studies of specific systems quoted below. Variable order concominants have drawn some attention as well, cf. Naber (2004) and Ramirez and Coimbra (2009). Recent studies bespeak the potential purport of the latter operators as a modelling tool for systems evincing a time dependent dispersion power $\langle r^2 \rangle \sim t^{\gamma(t)}$.

One group of applications manifests distinct scales $\gamma$ at well defined periods of time, i.e. a piecewise constant approximation of $\gamma(t)$ is a practical approach. An example thereof is a time limited process in a finite domain, as undergone by molecules in biological media (Reynolds, 2005; Bakalis et al., 2015), often with an auxiliary signalling reaction triggering an essential change in the spatial structure of the diffusing molecules or local medium (Cabal et al., 2006; Torreno-Pina et al., 2016). McKinley et al. (2009) construct a flexible model in the field of rheology, and Meerschaert et al. (2013) present a more formal framework.

Another group of applications employs a continuous exponent $\gamma(t)$. Sun et al. (2009) give examples of numerical solutions with a linear function in $t$ (as well as exponents depending on variables other than time). Saxton (1997) examines the distribution of diffusion coefficients in single particle tracking and demonstrates how statistically the apparent mean square displacement $\langle r^2 \rangle$ can be highly non-linear. The same author discusses a smooth cross-over between two regimes with constant $\gamma$ and compares to non-transient diffusion, connecting the results to experimental measurement techniques (Saxton, 2007). At times $\gamma$ and the conforming order of the diffusion equation are noted to depend on system variables such as concentration (Chen et al., 2013) or temperature (Morgan and Spera, 2001), however ultimately when the mean square displacement is measured, the exponent $\gamma$ will be time-dependent.

In light of the above, variable order fractional equations promise a significant advance in questions of correct interpretation of experimental measurements and juxtaposition of various particle tracking techniques. To date studies presented numerical solutions that could be compared to classic cases or fitted to experimental results, but offered little analytical insight. An analytical solution to a paradigm system, explicating the temporal evolution subject to transitions between disparate diffusive regimes and possible new behaviour thereupon, will

be a valuable step. This study focusses on a phenomenological reaction – diffusion system with an aim to relax the restriction of a constant order temporal derivative (mean square displacement growth power), thereby permitting the description of cross-over from regular diffusion to sub-diffusion and between sub-diffusive regimes.

## 2. Gierer-Meinhardt model

The reaction – diffusion system in question was first proposed by Gierer and Meinhardt (1972) and describes the interaction of two chemical species: an activator component that encourages the reaction process and an inhibitor, suppressing the rate thereof. When the diffusivity ratio between the components is asymptotically small with the reaction terms appropriately scaled, the system possesses a solution in the form of a set of spikes, i.e. localised spots of high concentration. With a fixed index $\gamma$ these solutions were obtained by Iron et al. (2001) for regular diffusion, $\gamma = 1$, and by Nec and Ward (2012) for sub-diffusion, $0 < \gamma < 1$. Here it is proposed to endow the problem with time variability of the anomaly index $\gamma$ that is also the order of the partial differential equations, but in a way that still admits of a solution.

On a finite, one-dimensional domain with no flux boundaries the unified model reads

$$\partial_t^\gamma a = \epsilon^{2\gamma} a_{xx} - a + \frac{a^p}{h^q} \qquad -1 < x < 1\,, \quad t > 0\,, \tag{2a}$$

$$\tau_o\, \partial_t^\gamma h = h_{xx} - h + \epsilon^{-\gamma} \frac{a^m}{h^s} \qquad -1 < x < 1\,, \quad t > 0\,, \tag{2b}$$

$$a_x(\pm 1, t) = h_x(\pm 1, t) = 0\,, \qquad a(x,0) = a_0(x)\,, \qquad h(x,0) = h_0(x)\,, \tag{2c}$$

where $a(x,t)$ and $h(x,t)$ are the activator and inhibitor concentrations, respectively. Here $0 < \epsilon \ll 1$, $\tau_o > 0$, the quadruple of reaction exponents $(p, q, m, s)$ satisfies

$$p > 1, \quad q > 0, \quad m > 0, \quad s \geqslant 0, \quad \frac{p-1}{q} < \frac{m}{s+1}, \tag{2d}$$

and the index $\gamma$ ranges $0 < \gamma \leqslant 1$. When $\gamma = 1$, system (2) comprises two conventional partial differential equations. When $0 < \gamma < 1$, the derivative of order $\gamma$ is defined (for a univariate function) as

$$\frac{d^\gamma}{dt^\gamma} f(t) = -\frac{1}{\Gamma(-\gamma)} \int_0^t \frac{f(t) - f(t-\zeta)}{\zeta^{\gamma+1}}\, d\zeta, \qquad 0 < \gamma < 1, \tag{2e}$$

wherein $\Gamma$ denotes the Gamma function. Further detail on this operator can be found in Elliot (1993) and Nec and Ward (2012). Since the integration is with respect to $\zeta$, it is forthwith admissible to extend the order to be a time dependent function $\gamma(t)$. Some forms of memory operators include differentiation with respect to $t$ or imbed the delay directly into the order through the dependence $\gamma(t-\zeta)$, therefore requiring a more careful generalisation,

cf. Ramirez and Coimbra (2009). Henceforth the anomaly index is deemed to be a function of time, designated thus explicitly $\gamma(t)$ or merely $\gamma$ for simplicity.

For a constant $\gamma$ the spike solution is constructed by the method of matched asymptotic expansions (Iron et al., 2001; Nec and Ward, 2012). On an infinite domain a similar construction is possible (Nec, 2016b). One of the tacit assumptions of this classic method is that the partial differential equations are of a fixed order, as are the concomitant asymptotic scales, together admitting a reduction to a system of non-linear algebraic equations for the spikes' heights and ordinary differential equations for the drift of loci. As shown hereinafter however, this reduction can be extended to the case of multiple transitions between a sequence of arbitrary orders within the range $0 < \gamma \leqslant 1$ at equally arbitrary cross-over moments.

## 3. A pattern of $n$ spikes

Consider an $n$-tuple of spikes centred at a set of arbitrary loci $x_i$, $\{i = 0, \ \dots \ , n-1\}$. Classically the outer solution for the activator away from the loci $x_i$ is the trivial quiescent state $a(x,t) \equiv 0$, whereas for the inhibitor $h(x,t)$ expand

$$h \sim h^{(0)}(x,t) + o(1). \tag{3}$$

Within a narrow region about the locus the inner spatial variable $y_i \stackrel{\text{def}}{=} (x - x_i)\Big/\epsilon^{\gamma(t)}$ is required to make the differential term on the right hand side in (2a) of order $\mathcal{O}(1)$. The corresponding slow time variable $\tau = \epsilon^{\alpha(t)}t$. The temporal scale $\alpha$ is determined below. The inner asymptotic solutions are set as

$$A_i(y_i,\tau) = a\Big(x_i + \epsilon^{\gamma(t)}y_i, \epsilon^{-\alpha(t)}\tau\Big) \sim A_i^{(0)}(y_i,\tau) + \epsilon^{\gamma(\tau)}A_i^{(1)}(y_i,\tau) + \cdots \tag{4a}$$

$$H_i(y_i,\tau) = h\Big(x_i + \epsilon^{\gamma(t)}y_i, \epsilon^{-\alpha(t)}\tau\Big) \sim H_i^{(0)}(y_i,\tau) + \epsilon^{\gamma(\tau)}H_i^{(1)}(y_i,\tau) + \cdots \ . \tag{4b}$$

The unusual feature about (4) is the time dependence of the scales $\gamma$ and $\alpha$, as conventionally these are constant. It is imperative to substantiate when an expansion of this ilk is valid. Obviously, it is valid when $\gamma$ and $\alpha$ are constant. Observe that it is also valid for any step-like function:

$$\gamma(t) = \sum_j \gamma_j\Big\{\theta\big(t - t_{\times j-1}\big) - \theta\big(t - t_{\times j}\big)\Big\}, \qquad j = 1, 2, \dots \ , \tag{5}$$

wherein $0 < \gamma_j \leqslant 1$ are constant anomaly indices, $\theta(t)$ denotes the Heaviside step function, $t_{\times j}$ are the corresponding cross-over times satisfying $t_{\times j} > t_{\times j-1}$ and $t_{\times 0} = 0$ without loss of generality. With $\gamma(t) \equiv 1$ the diffusion mechanism is the regular Fickian diffusion entailing a linear growth of the mean square displacement in time $\langle r^2 \rangle \sim t$, recovering the classic model (Gierer and Meinhardt, 1972). With $0 < \gamma(t) < 1$ the dispersion is sub-diffusive, i.e. $\langle r^2 \rangle \sim t^{\gamma(t)}$. A plain, fixed order process is obtained with all $\gamma_j$ equal. A regular to anomalous transition is given by $\gamma_j = 1$, $0 < \gamma_{j+1} < 1$ and vice versa, whilst $0 < \gamma_j < 1$, $\gamma_j \neq \gamma_{j+1}$ yield transitions between distinct sub-diffusive regimes. At any cross-over moment

$t_{\times_j}$ the scales of the entire asymptotic series (4) will be instantaneously adjusted.

Albeit the non-linearity introduced into series (4) through the dependence $\epsilon^{\gamma(t)}$ forthwith precludes an extension to functions of a more generic nature, it is hereby conjectured that the spike solution will persist (albeit not be described by the series above) for smooth functions such that the changes in $\gamma(t)$ occur on a time scale much faster than $\tau$. For instance for an inner layer transition

$$\gamma(t) = \frac{\gamma_{j+1} - \gamma_j}{2} \tanh \frac{t - t_{\times_j}}{\varepsilon} + \frac{\gamma_{j+1} + \gamma_j}{2} \tag{6}$$

this requirement is mathematically expressed as $\varepsilon \ll \epsilon^{-\alpha}$, posing virtually no restriction on the inner layer width $\varepsilon$ since $\epsilon \ll 1$ and $\alpha > 0$, whilst an inner layer exists as such for $\varepsilon \sim \mathcal{O}(1)$ or $\varepsilon \sim o(1)$. Thence illatively follows that the functional form of $\gamma(t)$ is encumbered but little, in particular any temporal variation on $\mathcal{O}(1)$ scale will not interfere with the formation of the spike and its slow drift.

For the solution construction to hold formally it must be assumed that $\gamma(t)$ is a piecewise constant function as in (5). However, any reasonably behaved function $\gamma(t)$ might be discretised into a set of step-like segments. The combination of solutions will remain valid as long as $t \sim O(1)$ or higher, i.e. no attempt is made to seek a truly smooth evolution, or to express that more technically, the orders of magnitude are preserved. Small steps in $\gamma$ are permissible as long as the restriction on $t$ is observed. Figure 1 shows a possible discretisation to approximate the smooth function (6).

For any given segment the classic reduction yields the following algebraic-differential system (consult Nec and Ward (2012) for technical detail). The spikes' heights $H_i^{(0)}$ (leading order inner solution for the inhibitor) are governed by a set of non-linear equations

$$H_i^{(0)}(\tau) = -b_m \sum_{j=0}^{n-1} {H_j^{(0)}}^{\beta m - s} G(x_i; x_j)\,, \tag{7a}$$

where $G(x, x_i)$ is the Green's function

$$G(x; x_i) = \begin{cases} -\operatorname{csch} 2 \cosh(x_i - 1) \cosh(x + 1) & x < x_i \\ -\operatorname{csch} 2 \cosh(x_i + 1) \cosh(x - 1) & x > x_i \end{cases} \tag{7b}$$

and

$$b_m = \int_{\mathbb{R}} u^m \, dy\,, \tag{7c}$$

is a factor computed from the homoclinic $u(y)$

$$u(y) = \left(\frac{p+1}{2}\right)^{1/(p-1)} \operatorname{sech}^{2/(p-1)} \left(\frac{p-1}{2}\ y\right) \tag{7d}$$

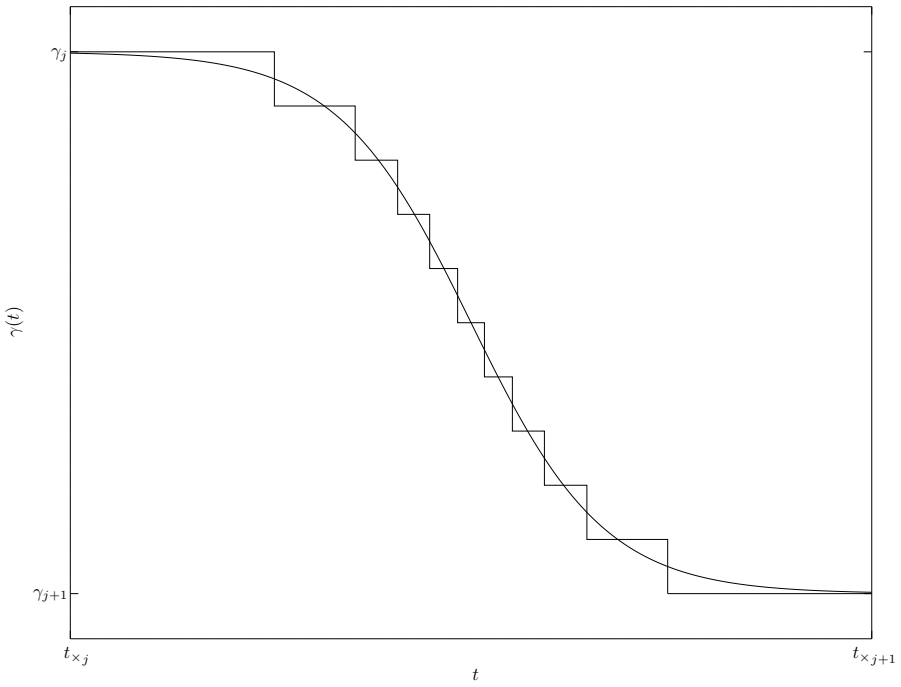


Figure 1: A valid discretisation example of a smooth cross-over.

that controls the spike's shape. In particular the leading order inner solution for the activator is given by

$$A_i^{(0)} = {H_i^{(0)}}^{\beta} u(y_i), \qquad \beta = \frac{q}{p-1}, \tag{7e}$$

whence $A_i(y_i, \tau)$ decays exponentially as $|y_i| \longrightarrow \infty$ and is localised in the vicinity of the spike locus $x_i$. The leading order outer solution for the inhibitor reads

$$h^{(0)}(x,t) = -b_m \sum_{i=0}^{n-1} {H_i^{(0)}}^{\beta m - s} G(x; x_i)\,. \tag{7f}$$

The spikes' loci $x_i(\tau)$ drift on the slow time scale $\tau = \epsilon^{\alpha} t$, $\alpha = \gamma + 1$, according to the differential system

$$\frac{dx_i}{d\tau}\left|\frac{dx_i}{d\tau}\right|^{\gamma-1} = \frac{q b_m f(p;\gamma)}{(p+1)H_i^{(0)}} \left\{ \frac{1}{2} {H_i^{(0)}}^{\beta m - s} \Big( G_x(x_i^-; x_i) + G_x(x_i^+; x_i) \Big) + \sum_{\substack{j=0 \\ j\neq i}}^{n-1} {H_j^{(0)}}^{\beta m - s} G_x(x_i; x_j) \right\}, \tag{7g}$$

$$f\Big(p;\gamma(t)\Big) \equiv \int_{\mathbb{R}} u^{p+1}\,dy \Bigg/ \int_{\mathbb{R}} u'(y)\mathfrak{D}_y^{\gamma}u\,dy\,, \tag{7h}$$

$$\mathfrak{D}_y^{\gamma}u(y) \equiv \frac{1}{\Gamma(-\gamma)}\ \operatorname{sgn}\frac{dx_i}{d\tau}\int_0^{\infty}\left\{u(y)-u\left(y+\xi\ \operatorname{sgn}\frac{dx_i}{d\tau}\right)\right\}\frac{d\xi}{\xi^{\gamma+1}}\,. \tag{7i}$$

With regular diffusion $f(p;1)=2(p+1)/(p-1)$, equation (7h) being a fractional generalisation thereof. Operator (7i) ostensibly distinguishes between leftward and rightward drift, thus breaking the symmetry of motion on either side of an equilibrium point. This is an explicit aftermath of the memory inherent to all temporal fractional derivatives. Nonetheless no actual asymmetry ensues, since the operator's only appearance is in the second integral in (7h), acting on the even function $u(y)$, in conjunction with the odd function $u'(y)$, so that the factor $f\big(p;\gamma(t)\big)$ does not depend on $\operatorname{sgn} x_i'(\tau)$. The function $\mathfrak{D}_y^{\gamma}u$ is neither even nor odd for $0<\gamma<1$ (consult figure 2). The functional dependence of $f(p;\gamma)$ is given in figure 3. At a cross-over time $t_{\times_j}$ the value will be instantaneously adjusted by a jump between respective values $\gamma_j$ and $\gamma_{j+1}$ on the curve corresponding to the same value of the kinetic exponent $p$. Bar the small interval of non-monotonicity for $p=2$ (uppermost curve in figure 3), diminution in $\gamma$ will always entail an increase in $f(p;\gamma)$.

Albeit classically the foregoing asymptotic reduction (7) was devised for a constant $\gamma$, a painstaking checking verifies its validity for a piecewise constant function $\gamma(t)$. This result is not altogether trivial, because whilst the inner spatial scale involves the compound $\epsilon^{\gamma}$, the slow time scale involves $\epsilon^{\alpha}$ with $\alpha=\gamma+1$, whence a jump in $\gamma$ cannot be forthwith absorbed in $\epsilon$. By and large system (7) permits a qualitative understanding of a variable order dynamical system of a fractional order $\gamma(t)$: within the limitations of the asymptotic theory unifying an arbitrary sequence of piecewise constant segments of $\gamma(t)$, it shows analytically that the variable order will not have an overwhelming impact on the nature of the solutions. Given that from a mathematical point of vantage relaxing the constraint of a fixed order is devastating to the application of traditional solution and analysis tools, and at the outset might lead to unpredictable results, this insight supports the physical soundness of variable order models. Past computational works showed examples of this inference, e.g. Sun et al. (2009); Chen et al. (2013), however with the Gierer-Meinhardt model a more formal substantiation is possible. Moreover, owing to the generic nature of the piecewise constant discretisation, it is safe to surmise that for most systems possessing asymptotic solutions of any kind the same procedure will conform to a valid description for an arbitrary piecewise constant sequence of orders. In addition it is illustrated hereinafter for specific spike constellations that a discretisation within the delineated limits of the presented theory yields a phase plane trajectory remarkably smooth visually, i.e. a piecewise constant sequence provides a good approximation without exacting the toll of a full numerical simulation. This last feature pertains solely to the Gierer-Meinhardt model, of course, and cannot be extended illatively to other dynamical systems.

System (7) is expected to be accurate by comparison to the full system (2) up to the

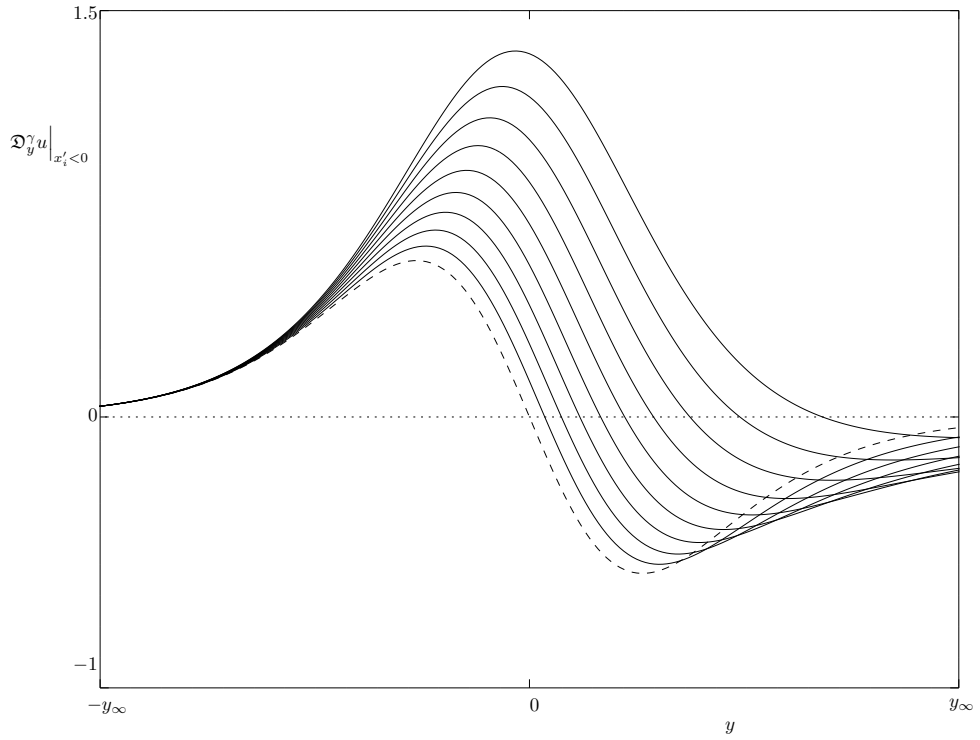


Figure 2: Function $\mathfrak{D}_y^\gamma u$ with the fractional operator $\mathfrak{D}_y^\gamma$ defined in (7i) for equally spaced $0.1 \leqslant \gamma \leqslant 0.9$ (solid curves, neither even nor odd functions) generalising $u'$ (dashed curve, odd function). The computation was performed for $\dfrac{dx_i}{d\tau} < 0$ and $p = 2$ upon regularisation of (2e) via integration by parts twice. The infinite bound of the integral was truncated at $3y_\infty$. Qualitatively similar results were obtained for $2 \leqslant p \leqslant 5$. Cf. figure 1 of Nec and Ward (2012), computed to higher accuracy here for expositional purposes.

order of the correction term in series (4), i.e. $\mathcal{O}\Big(\epsilon^{\gamma(\tau)}\Big)$. The concomitant error with regular diffusion is $\mathcal{O}(\epsilon)$. Similar reduced reaction– diffusion systems with regular diffusion have been shown to manifest excellent agreement with the full partial differential system, insofar as to predict correctly the onset of instability, cf. Sun et al. (2005) and Tzou et al. (2011). In stark contrast to integer order equations, partial differential equations of a fractional order, even without singular perturbations, require custom devised schemes, since conventional schemes have proved to baffle the regular notions as regards consistence, stability and accuracy (Meerschaert and Tadjeran, 2004). These difficulties are caused by the presence of memory, having at times unpredictable interference with other terms in the equations to be solved. In addition, time fractional operators contain integrals with singular kernels. Without exception successfully implemented schemes circumvented this fundamental quandary by regularising the operator. The modification involved either a change in the kernel, such as Caputo's derivative, several examples of which appear in Ramirez and Coimbra (2009), or addition of an initial term (Henry and Wearne, 2000) or both (Sun et al., 2009). Defi-

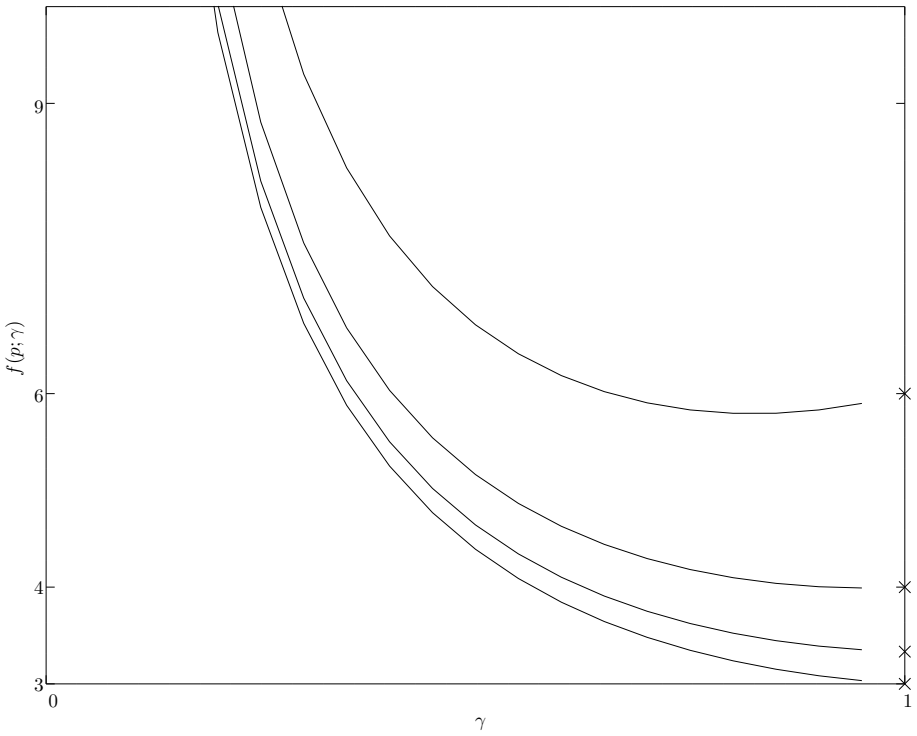


Figure 3: Factor $f(p;\gamma)$ for equally spaced $2 \leqslant p \leqslant 5$ computed for $\frac{1}{10} \leqslant \gamma \leqslant \frac{9}{10}$. Cross marks show the normal values $2(p+1)/(p-1)$. $f(p;\gamma) \longrightarrow \infty$ at the stagnation limit $\gamma \longrightarrow 0^+$. Cf. figure 3 of Nec and Ward (2012), computed to higher accuracy here for expositional purposes.

nition (2e) is not regularised, its particular form essential to preserve basic equilibrium and spectrum related properties of (2) as a dynamical system (more detail can be found in Nec (2016b)). Thus a numerical solution of (2) is impossible with standard computational means. Nonetheless, the error bound above can be used to calculate the maximal value of $\epsilon$ that would ensure the solution given by (7) not exceed the corresponding error in the normal system by taking $\min \gamma(\tau)$.

## 4. Quasi-equilibrium solutions

System (7) is the reduction of (2) at the limit $\epsilon \longrightarrow 0$. Different constellations of spikes were investigated to elucidate the effect of anomaly index transition on the drift toward equilibrium. Equation (7g) is a somewhat unconventionally written ordinary differential equation that can be cast into a better amenable to numerical integration form by $x_i'(\tau)\left|x_i'(\tau)\right|^{\gamma-1} = \operatorname{sgn} x_i'(\tau)\left|x_i'(\tau)\right|^{\gamma}$, and thence $x_i'(\tau)$ can be computed by evaluating the right hand side of (7g), whose sign determines $\operatorname{sgn} x_i'(\tau)$. Generally at every integration step the non-linear system (7a) must be solved, albeit some simple patterns permit an explicit solution. In

the classic Runge-Kutta procedure employed here or other predictor-corrector methods (7a) must be solved for all intermediate predictor steps as well.

A more fundamental peculiarity of (7g) is that the integration variable $\tau$ relates to the physical time $t$ through $\tau = t\epsilon^{\gamma(t)+1}$, therefore changing scale at every cross-over point $t_{\times j}$, prescribed by equation (5). In praxis without lost of generality every interval characterised by a fixed value $\gamma_j$ was integrated with $\tau$ initialised to zero and $\Big(x_i, H_i^{(0)}\Big)$ – to the values reached at the end of the preceding interval. The full variable $\tau$ was made monotonic upon completion of integration by addition of $\tau_{\times j} = t_{\times j}\epsilon^{\gamma_j+1}$.

Infra solutions are presented for two groups of transition scenarios. The first category examines a sequence of significant jumps in $\gamma$ with the purpose to exemplify the extent of abruptness in the pattern's response with respect to relative velocity of the spikes and their heights; demonstrate the variability of possible response behaviours; present non-intuitive or non-monotonic response to certain parameters; identify typical mechanisms responsible for pattern evolution that might be considered advantageous for a natural system, such as a capability of fast equilibration or quick non-linear excursions before attainment of equilibrium. The second category pertains to the smooth cross-over. Function (6) was used with the corresponding piecewise constant sequence in figure 1. Despite the coarseness of this discretisation all evolution trajectories appeared absolutely smooth. Thus only a concise sample is shown depicting this observation.

### *4.1. Single spike*

With $n = 1$ equation (7a) is forthwith soluble for the spike height as a function of the locus location $x_0$

$$H_0^{(0)} = \Big( - b_m G(x_0, x_0)\Big)^{-1/(\beta m - s - 1)}, \tag{8a}$$

whereby the differential equation (7g) can be integrated in closed form for $\gamma = 1$ to yield

$$\frac{-4q\tau}{p-1} = \ln \frac{\sinh(2x_0)}{\sinh(2x_0(0))} + \frac{1}{2}\cosh(2)\ \ln \frac{\Big(\cosh(2x_0) - 1\Big)\Big(\cosh(2x_0(0)) + 1\Big)}{\Big(\cosh(2x_0) + 1\Big)\Big(\cosh(2x_0(0)) - 1\Big)} \tag{8b}$$

or numerically for $0 < \gamma < 1$. Moreover, for any $\gamma$ the sole fixed point $x_0 = 0$ is stable, allowing to replace $\operatorname{sgn} x_i'(\tau) = -\operatorname{sgn} x_i$. From (7g) it is readily inferred that the only effect of $\gamma$ is the speed wherewith the spike approaches equilibrium. What is less immediate is whether a change in $\gamma$ incurs magnification or diminution of said speed. The magnitude of the right hand side of (7g) is below unity for any practical values of parameters, exclude for instance extremely small $\gamma$ since $\lim\limits_{\gamma \longrightarrow 0^+} f(p;\gamma) = \infty$. Thereby $x_i'(\tau)$ will involve this quantity's $1/\gamma > 1$ power for any $0 < \gamma < 1$. Bar a narrow region just below $\gamma = 1$ for $p = 2$, $f(p;\gamma)$ is a descending function of $\gamma$ (figure 3). Therefore the $1/\gamma > 1$ power and growth of $f(p;\gamma)$ are opposing influences, begetting the following behaviour: for a small increase in $f$, i.e. $\gamma$ slightly below unity, the spike will slow down somewhat, for more significant growth of $f$ it will speed up, whilst for small $\gamma$ its progress will again be delayed at the cross-over point

$t_\times$, this latter evolution occurring over a very narrow interval of $\gamma$. This is best exemplified when $f$ depends monotonically on $\gamma$, i.e. $p > 2$, although it is always correct. Figure 4 shows a typical example of this phenomenon.

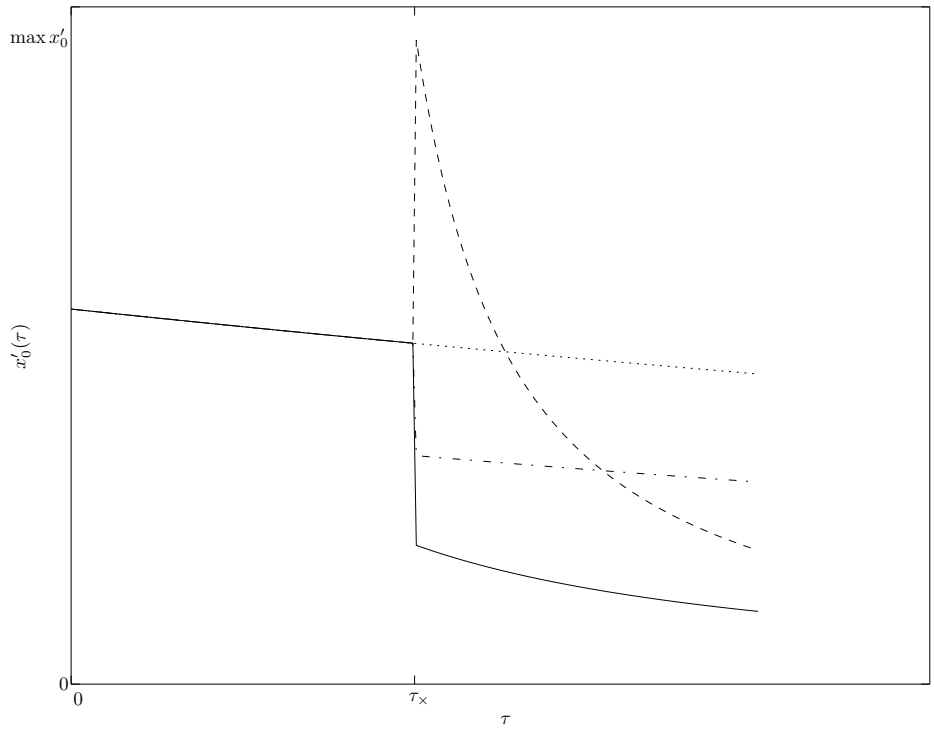


Figure 4: Anomaly dependent acceleration and delay phenomenon during the drift of a single spike: velocity $x_0'(\tau)$ for a transition scenario $\gamma(t < t_\times) = \gamma_1$, $\gamma(t > t_\times) = \gamma_2$ with $\gamma_1 = 1$ and $\gamma_2 = 1$ (dotted), $\gamma_2 = \frac{1}{2}$ (dash-dotted), $\gamma_2 = 0.0995$ (dashed) and $\gamma_2 = 0.099$ (solid). Note the non-monotonicity due to growth of $f(p;\gamma)$ with diminution of $\gamma$ counteracted by the $1/\gamma$ power in equation (7g). Other parameters used: $(p, q, m, s) = (3, 2, 2, 0)$, $t_\times = 10$, $\epsilon = \frac{1}{10}$, $x_0(0) = -\frac{1}{2}$. Qualitatively similar results obtained with $(p, q, m, s) = (2, 1, 2, 0), (2, 1, 3, 0), (4, 2, 2, 0)$.

With a single spike, or more generally any constellation with only one drift equation (more examples to be discussed hereinafter), the anomaly dependent acceleration or delay do not affect the trajectory traversed by the $i^{\text{th}}$ spike in the $\left(x_i, H_i^{(0)}\right)$ plane. The slow time variable $\tau$ parametrises this trajectory, hence transitions between different values of $\gamma$ impact solely the velocity of the spike motion, as visualised in figure 5. In light of the above a general conclusion follows that for this degenerate pattern additional transitions will not result in worthy of investigation phenomena.

### *4.2. Pair of spikes*

A well explored constellation is the symmetric pattern, where the premise of reflective symmetry $x_0 < 0$, $x_1(\tau) \equiv -x_0(\tau)$ entails equal heights $H_0^{(0)}(\tau) \equiv H_1^{(0)}(\tau)$ (Iron et al., 2001; Nec and Ward, 2012; Nec, 2016a). System (7) effectively reduces to one forthwith soluble

non-linear equation and one ordinary differential equation, whose closed form solution for $\gamma = 1$ is very similar to (8) and omitted here. Illatively from the single spike case, this pattern is not interesting as regards transient phenomena due to variable anomaly indices, as the trajectories are invariant albeit the parameterisation differs. Therefore it behoves one to centre the attention on asymmetric arrangements, whereat system (7) comprises two pairs of coupled equations.

The effect of varying anomaly index is better evident when initially the loci are positioned significantly away from the symmetric constellation. Figure 6 shows the trajectories of $H_i^{(0)}(x_i)$, $i = \{0, 1\}$ for a scenario of five distinct anomaly indices. Note the non-monotonicity of the left spike's height adjustment: with diminishing $\gamma$ in the first two transitions the spike grows higher, then lower as $\gamma$ decreases further at the third transition, followed by slight growth with $\gamma$ returning to normal. The response of the right spike does not manifest obvious conforming evolution, as it is located farther from its equilibrium point, its motion centred on attainment thereof. In particular the left spike overshoots the equilibrium height for a spell to compensate for the right spike's position. Indeed eventually the two spikes are similarly close to the respective equilibria (compare locations at trajectory ends), albeit never symmetric. Juxtaposition with the propagation without anomaly reveals a twofold impact: the left spike, initially situated near its equilibrium point, would have achieved the equilibrium height very slowly but for the transition, whilst the right spike would have been nowhere close to the equilibrium position or height within the same time frame. Thus the transition to anomaly might be a powerful mechanism to speed up the pattern's equilibration.

With a set of kinetic exponents corresponding to higher values of $\beta$, and thence a stronger non-linearity, it is also possible to obtain a trajectory that includes an excursion away from equilibrium before converging thereto. This occurs when the initial heights of the two spikes are on different sides of the equilibrium value. Nonetheless here too the equilibration is essentially faster with anomaly. Figure 7 depicts a situation of this ilk.

### *4.3. Triple of spikes*

The symmetric arrangement $\Big(x_0(\tau), x_1(\tau), x_2(\tau)\Big) \equiv \Big(x_0(\tau), 0, -x_0(\tau)\Big)$ again effectively reduces system (7) to a single differential equation of the autonomous type, to wit no differences in trajectories $\Big(x_i(\tau), H_i^{(0)}(\tau)\Big)$ will ensue regardless of the parameterisation in $\tau$. Thus, as before, only asymmetric constellations are of interest. Figure 8 gives a typical equilibration trajectory. Interesting phenomena to observe are earlier approach towards the equilibrium height $H_{\text{eq}}^{(0)}$ for all three spikes with a transition to sub-diffusion, possible overshooting of $H_{\text{eq}}^{(0)}$ whilst drift with regular diffusion begets no such occurrence (right spike $x_2$), and further excursion from $H_{\text{eq}}^{(0)}$ by comparison to the regular trajectory (central spike $x_1$). Figure 9 depicts the evolution for a combination of kinetic parameters that incur initial height on different sides of the equilibrium value $H_{\text{eq}}^{(0)}$. With this set of parameters, corresponding to a higher value of $\beta$, it is possible to obtain an overshooting of equilibrium by the normal trajectory, but not the anomalous one (left spike, $x_0$), as well as a considerably delayed overshooting (right spike, $x_2$).

*4.4. Quadruple of spikes*

For any $n > 3$ a symmetric arrangement of either even

$$\Big(x_0(\tau), x_1(\tau), \dots \quad x_{n/2-1}(\tau), -x_{n/2-1}(\tau) \quad \dots, -x_1 - x_0\Big)$$

or odd

$$\Big(x_0(\tau), x_1(\tau), \dots \quad x_{(n-1)/2-1}(\tau), 0, -x_{(n-1)/2-1}(\tau) \quad \dots, -x_1 - x_0\Big)$$

number of spikes system (7) will require the solution of $\left\lfloor \frac{n}{2} \right\rfloor$ non-linear equations for the spike heights and an equal number of respective drift differential equations. In this sense a pattern of four spikes is the first case, where a non-smooth trajectory $\left(x_i(\tau), H_i^{(0)}(\tau)\right)$ is expected with a symmetric initial state. Figure 10 shows such an example.

With an asymmetric initial state similar phenomena are obtained as with $n \leqslant 3$: considerable excursions, faster occurring changes in spike height and marked non-monotonicity. Rather consistently the spikes drift a larger distance than subject to an uninterrupted normal diffusion regime. A typical example is given in figure 11. In light of these observations constellations of $n > 4$ are expected to introduce more variability within the available degrees of freedom, but reveal no qualitatively new phenomena. It is noteworthy that the same set of kinetic exponents that for pairs and triples engendered less typical evolution, with $n = 4$ failed to yield an equilibrated pattern (with initial conditions and all transition parameters identical to other sets used). This occurrence was further investigated and is discussed hereinafter.

Figure 12 illustrates the smoothness of phase plane trajectories for the same constellation and initial conditions, but a discretised transition sequence approximating a smooth crossover in figure 1. From the result it is seen that a full solution would not produce tangibly smoother curves, proving the soundness of the approximation procedure. The computation was performed for all foregoing constellations with a similar aftermath. The particular example shown was chosen due to well defined non-monotonicity in height evolution that was nonetheless traced smoothly.

## 5. Existence of solutions

System (7) is valid as long as $H_i^{(0)} > 0 \ \forall i$ and all $x_i$ are sufficiently far apart. Being a reduction of the full partial differential system (2) on the slow time scale $\tau$, (7) cannot track behaviour that breaches the assumptions of quasi-equilibrium.

One such event of relevance here is a termination of a solution branch due to a bifurcation. To the best of the author's knowledge this occurrence has not been formally explored in the algebraic-differential system associated with the spike solution in Gierer-Meinhardt model, albeit it has been observed in numerical simulations (Tzou, 2016). A constellation following a branch in the $2n$-dimensional space $\left(x_i, H_i^{(0)}\right)$, $i = \{0, \dots, n-1\}$ that terminates before the equilibrium point is reached, will not be able to equilibrate. Only simulation of the full partial differential system (2) can elucidate the shift to another solution branch and

possible changes in the constellation, a study beyond the ambit of the current analysis. The existence of a bifurcation and concomitant termination of the trajectories in each of the planes $\left(x_i, H_i^{(0)}\right)$ is an inherent property of the reduced Gierer-Meinhardt system and not the result of sub-diffusion or transitions between distinct values of the anomaly index, however a bifurcation might induce an earlier termination in the presence of anomaly or beget unbounded growth. Typical examples appear hereunder, and no attempt is made to map the parameter space effecting a bifurcation.

The first example is for a system with regular diffusion and no transitions, i.e. $\gamma \equiv 1$. Figure 13 shows the spike velocity $x_i'(\tau)$ and trajectories $H_i^{(0)}(x_i)$ for a quadruple of spikes. Whilst the velocity is finite, note that the slope at the terminus point $\tau_{\mathrm{trm}}$ becomes infinite, as does $\dfrac{d}{d\tau}H_i^{(0)}$. Nevertheless $x_i'(\tau)$ remains finite, as this is not a singularity of (7g). One must bear in mind the terminus is indeed attained – the integration ceases because (7a) possesses no solution, in contrast to the equilibration itself with its exponentially or algebraically slow approach towards the fixed point, or a finite time blow up, where computation becomes impractical.

If $\gamma$ is moderately small, a constellation might reach a branch terminus, whilst with $\gamma \equiv 1$ no bifurcation is encountered. An example of this is given in figure 14. This constellation is initialised identically to the one used in figure 11 with sets of kinetic exponents begetting no solution existence issues.

An unimpeded growth of $\left|x_i'(\tau)\right|$ might ensue for small values of $\gamma$, when the right hand side of (7g) exceeds unity in magnitude. Re-write the left hand side of (7g) as $\operatorname{sgn} x_i'\left|x_i'\right|^{\gamma}$, whence it is readily inferred that $1/\gamma$ begets a power growth. For instance, with the same set of parameters as in figure 14, if another cross-over moment is added anywhere in the range $t_{\times 1} < t_{\times 2} < t_{\mathrm{trm}}$ and $\gamma_3 < \gamma_2$, the solution grows beyond the computer's handling ability within a few integration steps after the transition.

## 6. Discussion

The infinitesimally narrow spike solution, existing for the Gierer-Meinhardt model with both regular diffusion ($\gamma = 1$) and sub-diffusion ($0 < \gamma < 1$), persists when the index $\gamma$, traditionally a constant, is a piecewise constant function. To wit, the validity of the asymptotic spike pattern extends to the situation when the system undergoes transitions between regimes, whose mean square displacement evolution $\langle r^2(t)\rangle \sim t^{\gamma}$ is characterised by distinct exponents. The number of transition points as well as their cross-over timings $t_{\times j}$ and corresponding anomaly indices $0 < \gamma_j \leqslant 1$ are arbitrary.

At each transition $\gamma_j \longrightarrow \gamma_{j+1}$ occurring at $t_{\times j}$, $j = 1, 2, \ldots$, the drift velocity $x_i'(\tau)$ has a jump discontinuity, therefore the spike height $H_i^{(0)}(\tau)$ and locus position $x_i(\tau)$ are continuous, but not smooth. Generally the non-smoothness is retained in the plane $\left(x_i, H_i^{(0)}\right)$, with the exception of trajectories $H_i^{(0)}(x_i)$ where $\tau$ is an arbitrary parameterisation variable, i.e. for those constellations that are effectively described by a sole non-linear equation for the

height and respective differential equation for locus drift, namely a single spike, a pair of symmetric spikes, and a triple with central spike at equilibrium $x_1 \equiv 0$ and outer spikes moving symmetrically. Thence for $n \leqslant 3$ only asymmetric initial states yield qualitatively distinct trajectories for a sequence of transitions by comparison to a constant $\gamma(t)$. For $n \geqslant 4$ both symmetric and asymmetric initial states give non-smooth trajectories in the locus position – spike height planes. Near the equilibrium points transitions occasion but small differences in velocity, therefore often the non-smoothness is virtually indiscernible.

The manifold alterations in the trajectory form range from minor and quantitative to qualitatively novel behaviour. Depending on the specific parameters chosen, a pattern might equilibrate significantly faster than with a single fixed anomaly index, be it normal or sub-diffusive; the spikes might drift a larger distance in the process; the spike height might reach a local maximum or minimum that would not have been attained without a series of transitions. Recollecting that the spike height conforms to reactant concentration in the original chemical model, these results bear on recent experimentally documented concepts related to reactions within such complex biological media as cell membranes, organelles and nuclei. The most prominent aftermath of permitting the conventionally constant anomaly index to vary in time is the instantaneous adjustment of the spike's velocity. This behaviour qualitatively corresponds to a number of scenarios. One is a concatenation of events, when a cascade of consecutive periods of molecule diffusion and subsequent reactions trigger each other in turn, each with its own physical characteristics due to the locality of each drifting cluster and ligands. When out of a set of identical diffusing molecules a sufficient number is bound at the target, the concentration of that reactant diminishes, signalling the next reaction in the chain and possible slowing down of the initial diffusion. Another is that docking of the designated molecules will trigger a fast removal of the remaining reactant, thereby requiring a significant acceleration of their spatial propagation. Yet another is diffusion through distinct media, like penetration in and out of a nucleus or a cell or within such systems as the lymphatic vessels and nodes, where multifarious stages can be characterised by different anomaly indices.

The findings presented are based on an asymptotic reduction of a system of partial differential equations of a fractional order. Ideally it is desirable to obtain a numerical verification in those parts of the parameter space, where the asymptotic solution is valid. Numerical solution of partial fractional differential equations is notoriously difficult and often defies conventional concepts of numerical analysis as regards consistence, accuracy and stability of schemes (Meerschaert and Tadjeran, 2004). Here the challenge due to the kernel singularity of (2e) is further compounded by an increase in the spike width with diminishing $\gamma$, whereby the interval of feasible values of $\epsilon$ is narrower than the concomitant expected for normal diffusion and integer order equations. Development of a suitable numerical scheme is an enduring problem and topic of future research. All past successful schemes resorted to a regularisation of the fractional operator, a course of action impossible here, given that the operator is needed in its current form for the spike pattern to exist as well as certain spectral properties to be retained.

The Gierer-Meinhardt system is a paradigmatic model, representing no particular natural application, but capable of reconstructing general observable phenomena. Whist having once

more proved a powerful pattern forming tool, the limitation of the solution obtained here is in the requirement that the anomaly index remain constant between any two transition points. Whilst a formally continuous variation of $\gamma$ might be a curious topic for future research, the posed theory was shown to yield evolution trajectories appearing visibly smooth when a smooth function $\gamma(t)$ was discretised into a sequence of step-like segments. The limitations on the validity of the presented asymptotic solution are not burdensome, therefore such discretisation is feasible for most reasonably behaved $\gamma(t)$. Moreover, the method itself is generic and might be easily adapted to unrelated dynamical systems, as long as an asymptotic solution with fixed scales is available. The degree of smoothness in the solution will depend on the particular system at hand. It is furthermore conjectured that for $\gamma(t)$ of an abrupt, yet continuous variation, for instance an inner layer as in (6) with $\varepsilon \ll 1$, away from the transition core the solution obtained herein will faithfully capture the dynamics, whilst in the vicinity thereof some delay in adjustment of the spike velocity will ensue, depending on the specific dependence of $\gamma(t)$. Perhaps an asymptotic solution might be furnished for certain forms of $\gamma(t)$ based on an independent small parameter describing the abruptness of transition. With an unrestricted variation, i.e. $\gamma(t)$ such that no regions can be approximated by a constant, a disparate method of solution will be required, as the current asymptotic approach becomes unfeasible.

The Gierer-Meinhardt system is further amenable to a generalisation involving a fractional Laplacian (spatial fractional derivative), thereby admitting solutions of spikes that propagate according to Lévy flights, a type of super-diffusion (Nec, 2012). Extension of the current analysis to include transitions between Lévy flights with distinct anomaly indices as well as between sub-diffusive to super-diffusive regimes is another future problem.

## References


Bakalis, E., Höfinger, S., Venturini, A., 2015. Crossover of two power laws in the anomalous diffusion of a two lipid membrane. J. Chem. Phys. 142, 215102.

Cabal, G. G., Genovesio, A., Rodrigues-Navarro, S., Zimmer, C., Gadal, O., Lesne, A., Buc, H., Feuerbach-Fournier, F., Olivo-Marin, J. C., Hurt, E. C., Nehrbass, U., 2006. SAGA interacting factors confine sub-diffusion of transcribed genes to nuclear envelope. Nature 441, 770–773.

Chen, W., Sun, H., Zhang, X., Korošak, D., 2010. Anomalous diffusion modeling by fractal and fractional derivatives. Comp. Math. Appl. 59, 1754–1758.

Chen, W., Zhang, J., Zhang, J., 2013. A variable-order time-fractional derivative model for chloride ions sub-diffusion in concrete structures. Frac. Calc. Appl. Analysis 16, 76–92.

Codling, E. A., Plank, M. J., Benhamou, S., 2008. Random walk models in biology. J. R. Soc. Interface 5, 813–834.

Eliazar, I., Klafter, J., 2011. Anomalous is ubiquitous. Annals of Physics 326, 2517–2531.

Elliot, D., 1993. An asymptotic analysis of two algorithms for certain Hadamard finite-part integrals. IAM J. Num. Analysis 13, 445–462.

Gierer, A., Meinhardt, H., 1972. A theory of biological pattern formation. Kybernetik 12, 30–39.

Henry, B. I., Wearne, S. L., 2000. Fractional reaction–diffusion. Physica A 276, 448–455.

Iron, D., Ward, M. J., Wei, J., 2001. The stability of spike solutions to the one-dimensional Gierer-Meinhardt model. Physica D 150, 25–62.

Klages, R., Radons, G., Sokolov, I. M., 2008. Anomalous transport: foundations and applications. Wiley-VCH, Weinheim.

McKinley, S. A., Yao, L., Forest, M. G., 2009. Transient anomalous diffusion of tracer particles in soft matter. J. Rheol. 53, 1487.

Meerschaert, M. M., Nane, E., Vellaisamy, P., 2013. Transient anomalous sub-diffusion on bounded domains. Proc. Amer. Math. Soc. 141, 699–710.

Meerschaert, M. M., Tadjeran, C., 2004. Finite difference approximations for fractional advection – dispersion flow equations. J. Comput. Appl. Math. 172, 65–77.

Metzler, R., Klafter, J., 2000. The random walk's guide to anomalous diffusion: a fractional dynamics approach. Physics Reports 339, 1–77.

Morgan, N. A., Spera, F. J., 2001. A molecular dynamics study of the glass transition in $CaAl_2Si_2O_8$: thermodynamics and tracer diffusion. American Mineralogist 86, 915–926.

Naber, M., 2004. Distributed order fractional sub-diffusion. Fractals 12, 23.

Nec, Y., 2012. Spike-type solutions to one dimensional Gierer-Meinhardt model with Lévy flights. Studies in Appl. Math. 129, 272–299.

Nec, Y., 2016a. Dynamics of spike solutions in Gierer-Meinhardt model with time dependent diffusivity. preprint.

Nec, Y., 2016b. Explicitly solvable eigenvalue problem and bifurcation delay in sub-diffusive Gierer-Meinhardtmodel. Euro. J. Appl. Math., doi:10.1017/S0956792516000012.

Nec, Y., Ward, M. J., 2012. Dynamics and stability of spike-type solutions to a one dimensional Gierer-Meinhardt model with sub-diffusion. Physica D 241, 947–963.

Oldham, K. B., Spanier, J., 1974. Fractional Calculus. Academic Press, New York.

Ramirez, L. E. S., Coimbra, C. F. M., 2009. On the selection and meaning of variable order operators for dynamic modeling. International J. Diff. Eq. 2010, 846107.

Reynolds, A. M., 2005. On the anomalous diffusion characteristics of membrane-bound proteins. Physics Letters A 342, 439–443.

Saxton, M. J., 1997. Single-particle tracking: the distribution of diffusion coefficients. Biophys. J. 72, 1744–1753.

Saxton, M. J., 2007. A biological interpretaton of transient anomalous subdiffusion. i. qualitative model. Biophys. J. 92, 1178–1191.

Sun, H., Chen, W., Chen, Y. Q., 2009. Variable-order fractional differential operators in anomalous diffusion modeling. Physica A 388, 4586–4592.

Sun, W., Ward, M. J., Russell, R., 2005. The slow dynamics of two-spike solutions for the Gray-Scott and Gierer-Meinhardt systems: competition and oscillatory instabilities. SIAM J. Appl. Dyn. Sys. 4(4), 904–953.

Torreno-Pina, J. A., Manzo, C., Garcia-Parajo, M. F., 2016. Uncovering homo- and hetero-interactions on the cell membrane using single particle tracking approaches. J. Phys. D: Appl. Phys. 49, 104002.

Tzou, J. C., 2016. private communication.

Tzou, J. C., Bayliss, A., Matkowsky, B. J., Volpert, V. A., 2011. Stationary and slowly moving localised pulses in a singularly perturbed Brusselator model. Euro. J. Appl. Math. 22(5), 423–453.

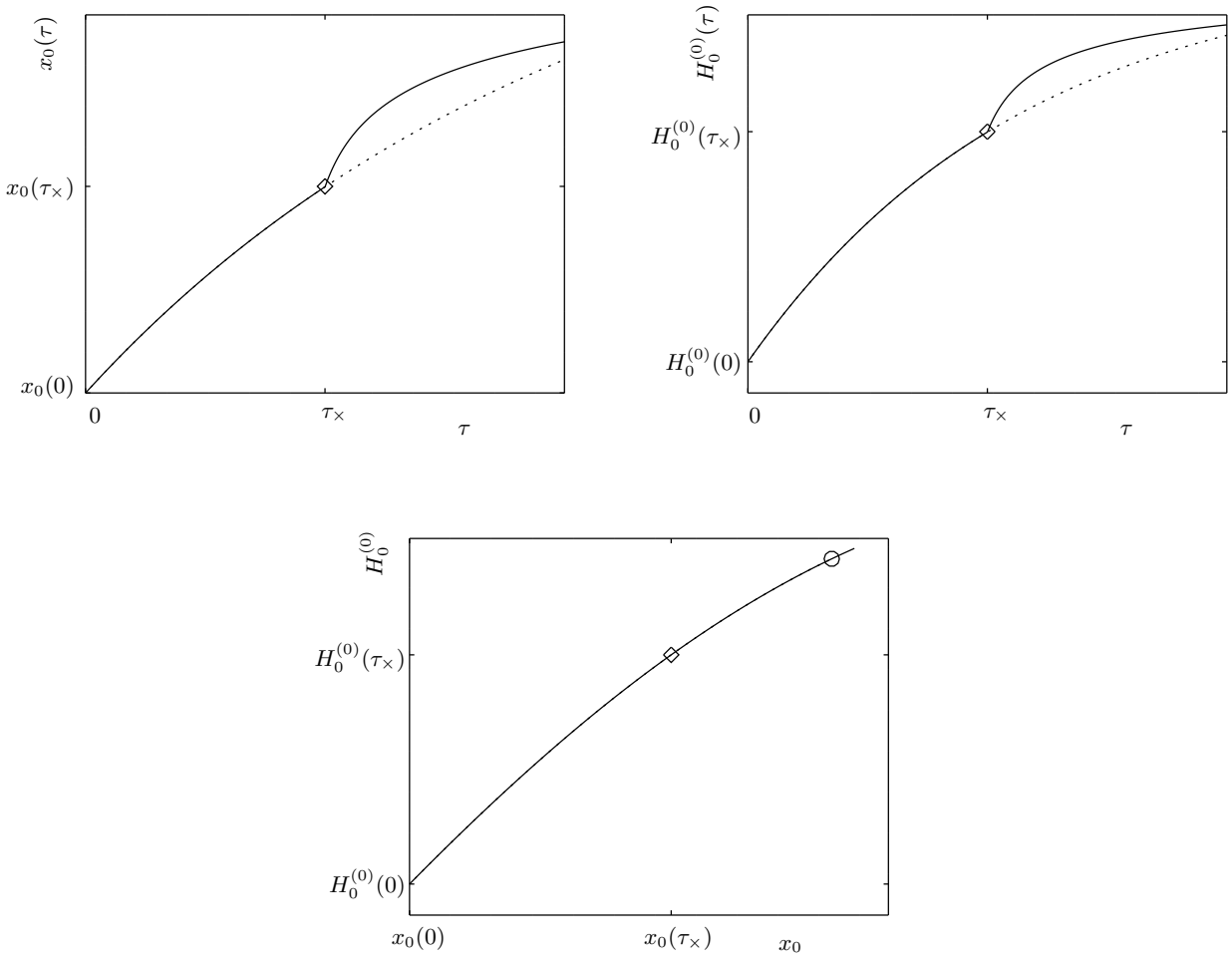


Figure 5: Trajectory parameterisation example for a single spike and transition scenario $\gamma(t < t_\times) = 1$, $\gamma(t > t_\times) = \frac{1}{5}$ (solid curves) and drift with no transition, $\gamma \equiv 1$ (dotted curves): locus position $x_0(\tau)$ (upper left panel), $H_0^{(0)}(\tau)$ (upper right panel) and $H_0^{(0)}(x_0)$ (bottom panel). Diamonds mark the cross-over moment $\tau_\times = t_\times \epsilon^{\gamma(t)+1}$ on all panels. Circle marks the end of the indistinguishable dotted curve on the bottom panel: from the upper panels it is obvious that the spike speeds up upon transition, therefore the solid trajectory (with transition) extends further than the dotted one (no transition). Other parameters used: $(p, q, m, s) = (3, 2, 2, 0)$, $t_\times = 50$, $\epsilon = \frac{1}{10}$, $x_0(0) = -\frac{3}{4}$. Qualitatively similar results obtained with $(p, q, m, s) = (2, 1, 2, 0), (2, 1, 3, 0), (4, 2, 2, 0)$.

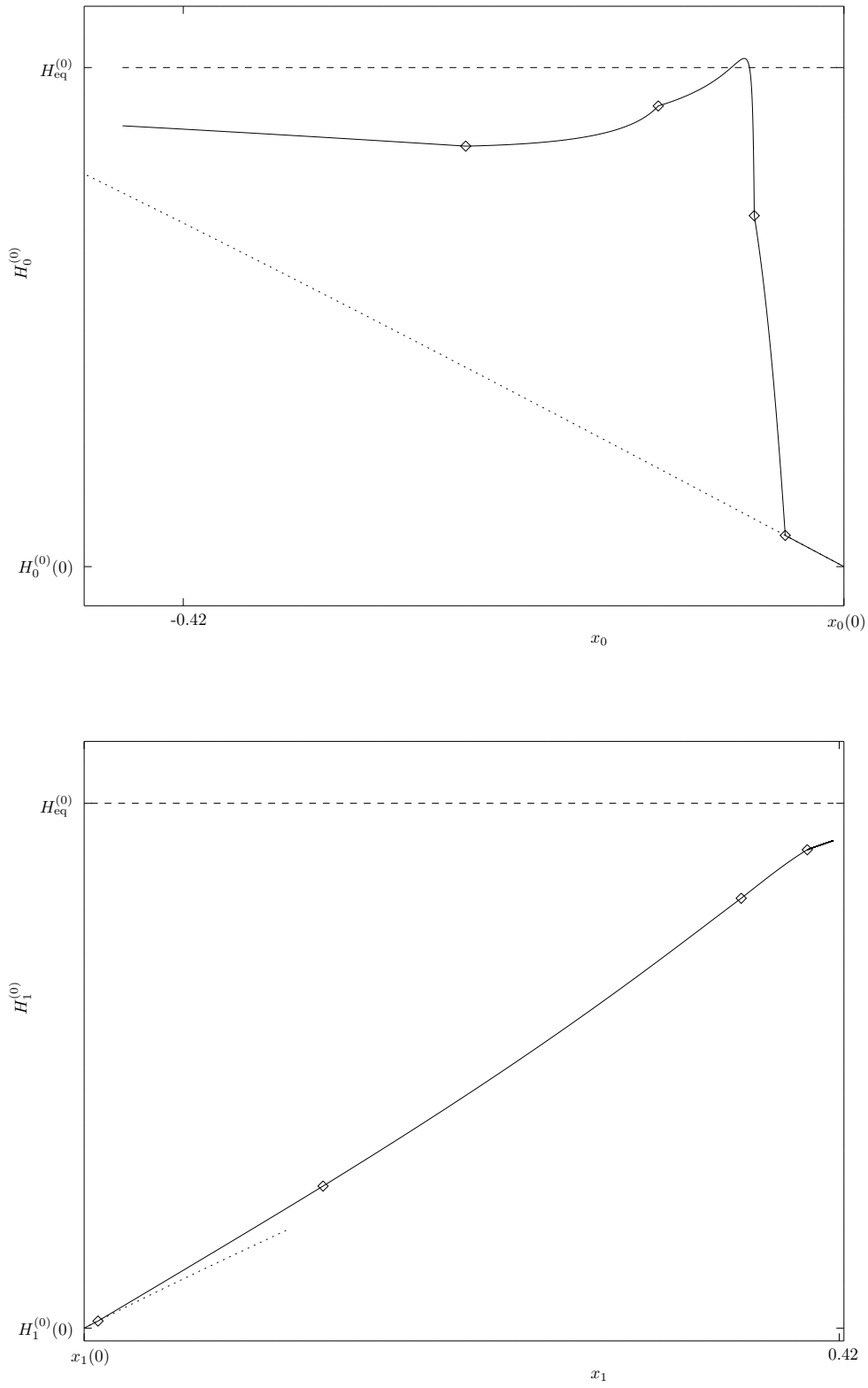


Figure 6: Trajectory parameterisation example for a pair of spikes and transition scenario of five intervals characterised by $\gamma = \left\{1, \frac{1}{4}, \frac{3}{20}, \frac{1}{10}, 1\right\}$ with cross-over moments $t_\times = \{1, 2, 6, 8\}$. Initial position is $\left(x_0, x_1\right) = \left(-\frac{2}{5}, \frac{1}{10}\right)$. Equilibrium position is $\left(x_0, x_1\right) = \left(-\frac{1}{2}, \frac{1}{2}\right)$. Equilibrium height, equal for both spikes, is marked by the dashed line. Dotted lines show the trajectory for $\gamma \equiv 1$ (in upper panel continuing beyond the frame given). Diamonds mark the cross-over moments $t_{\times j}$. Other parameters used: $(p, q, m, s) = (3, 2, 2, 0)$, $\epsilon = \frac{1}{10}$. Qualitatively similar results obtained with $(p, q, m, s) = (2, 1, 2, 0), (4, 2, 2, 0)$.

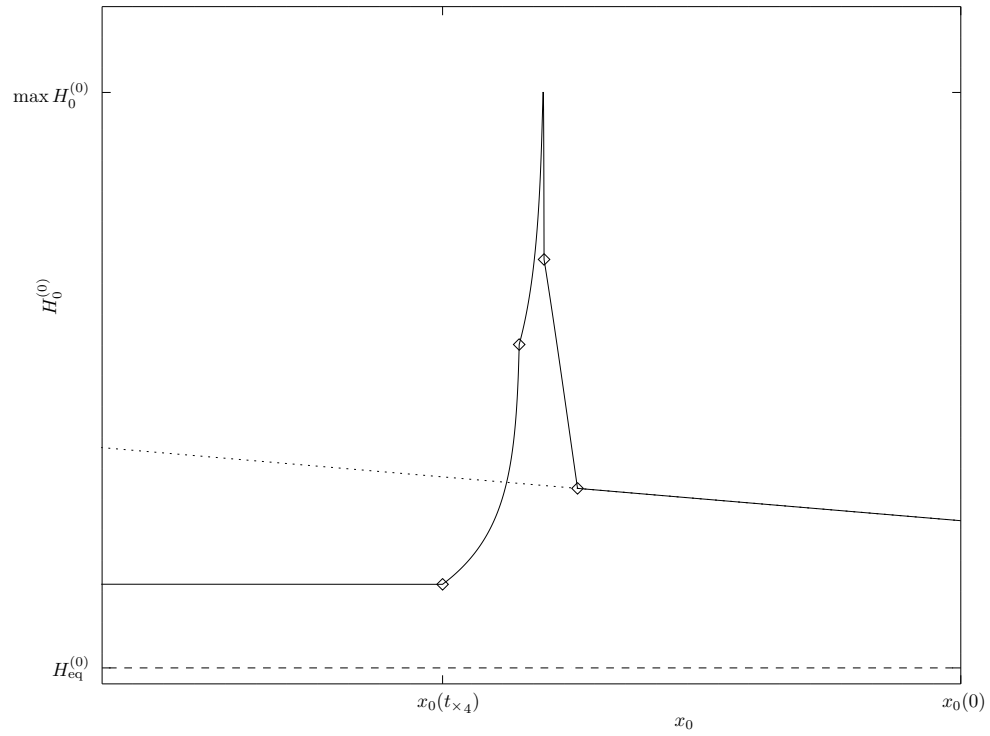
$\max H_0^{(0)}$
$H_0^{(0)}$
$H_{\rm eq}^{(0)}$
$x_0(t_{\times 4})$
$x_0(0)$
$x_0$

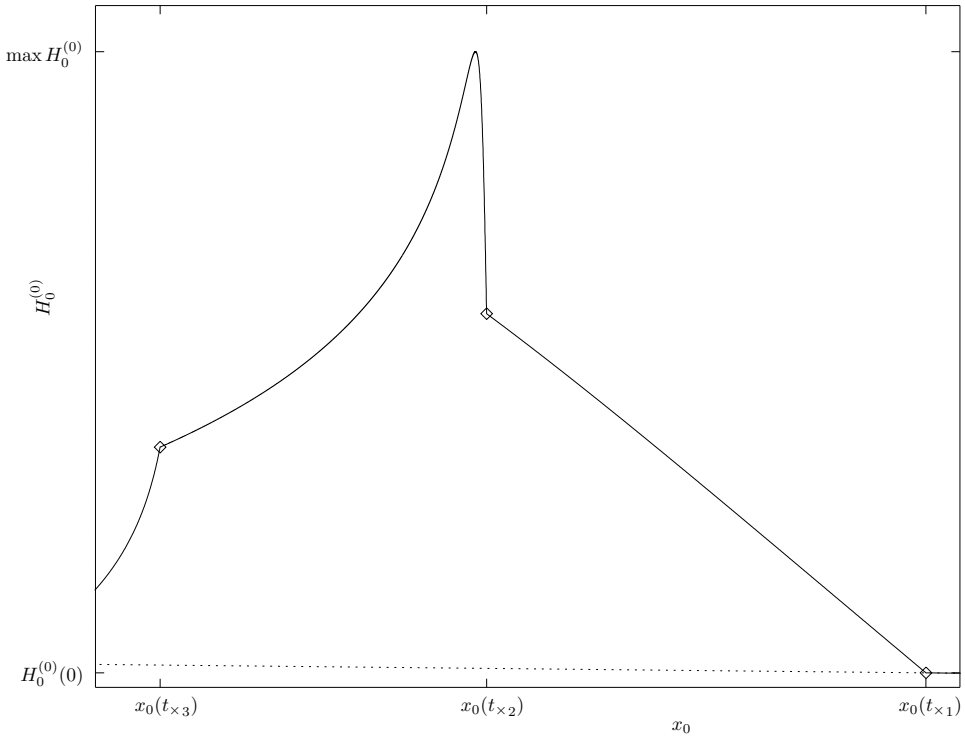
$\max H_0^{(0)}$
$H_0^{(0)}$
$H_0^{(0)}(0)$
$x_0(t_{\times 3})$
$x_0(t_{\times 2})$
$x_0(t_{\times 1})$
$x_0$

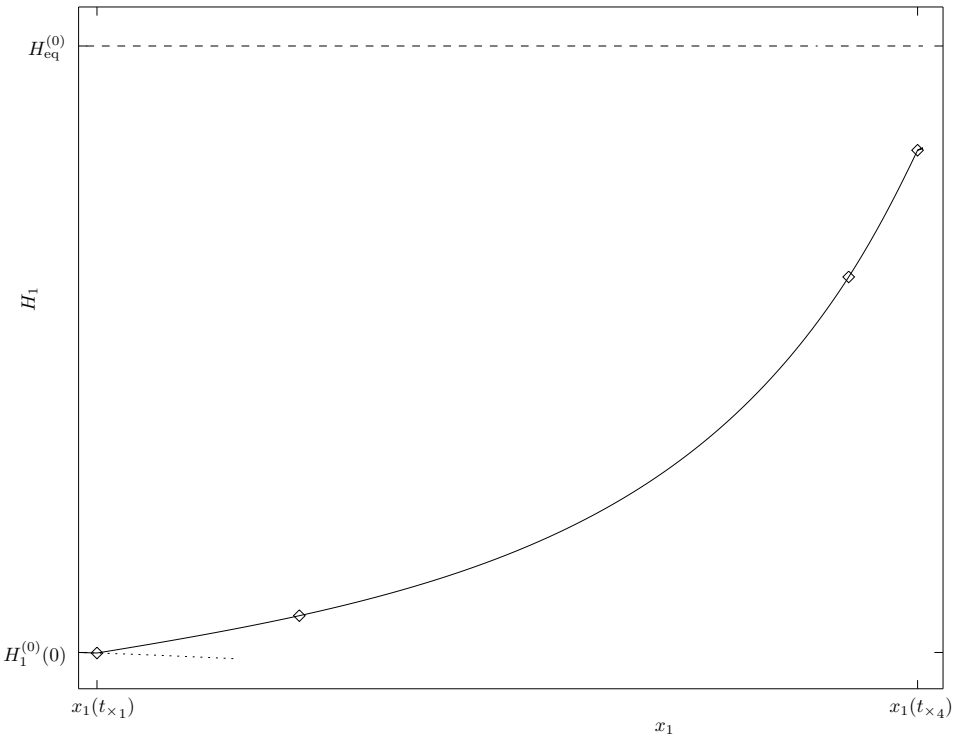


Figure 7: Example of non-monotonic equilibration for a pair of spikes with transition scenario of five intervals characterised by $\gamma = \left\{1, \frac{1}{4}, \frac{3}{20}, \frac{1}{10}, 1\right\}$ with cross-over moments $t_\times = \{1, 2, 6, 8\}$: left spike exhibits trajectory excursion away from equilibrium prior to convergence (upper panel, height peak vicinity enlarged in central panel), right spike's response is monotonic (lower panel). Initial position is $\left(x_0, x_1\right) = \left(-\frac{2}{5}, \frac{1}{10}\right)$. Equilibrium position is $\left(x_0, x_1\right) = \left(-\frac{1}{2}, \frac{1}{2}\right)$. Equilibrium height, equal for both spikes, is marked by the dashed line (observe left spike begins above equilibrium height, whilst right spike is below). Dotted lines show the trajectory for $\gamma \equiv 1$ (in upper and central panels continuing beyond the frame given). Diamonds mark the cross-over moments $t_{\times j}$. Other parameters used: $(p, q, m, s) = (2, 1, 3, 0)$, $\epsilon = \frac{1}{10}$.

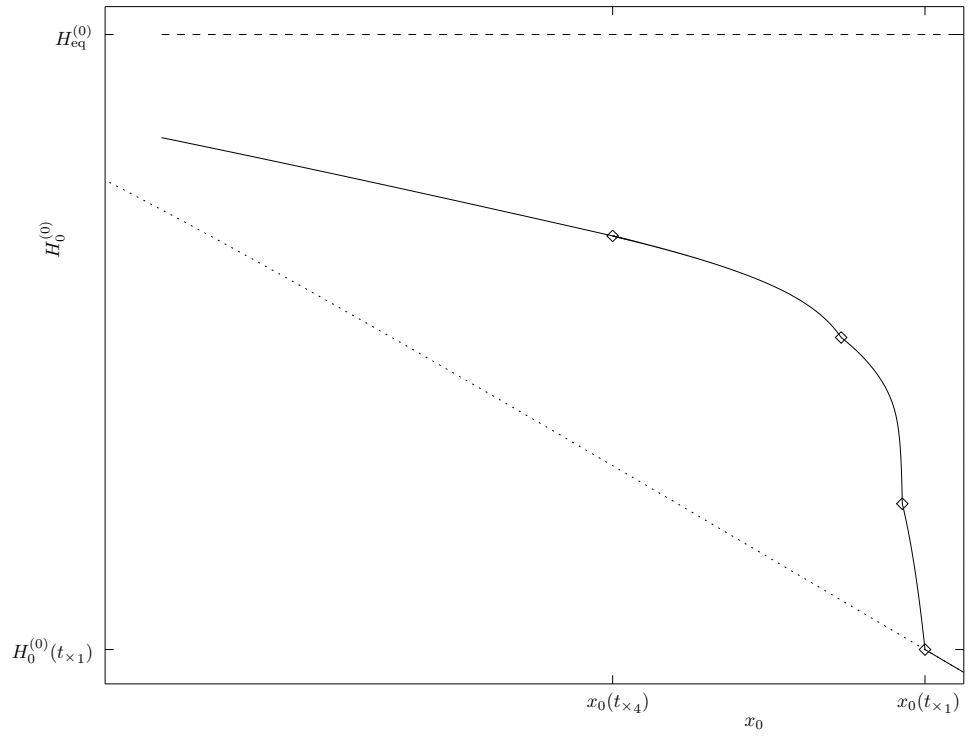
$H_{\rm eq}^{(0)}$
$H_0^{(0)}$
$H_0^{(0)}(t_{\times 1})$
$x_0(t_{\times 4})$
$x_0(t_{\times 1})$
$x_0$

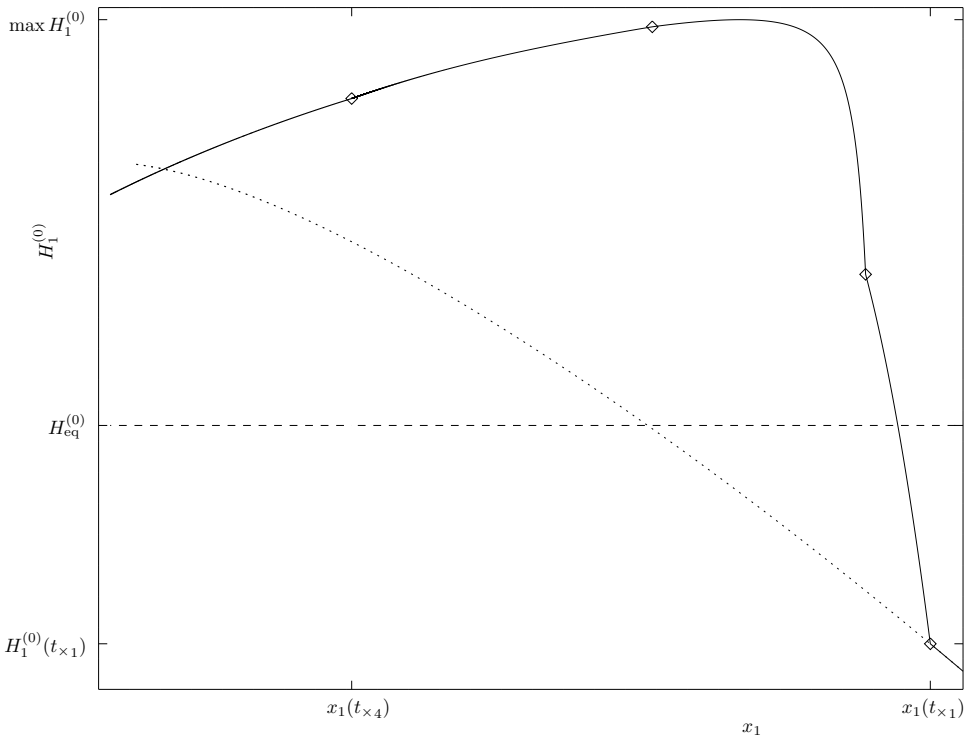
$\max H_1^{(0)}$
$H_1^{(0)}$
$H_{\rm eq}^{(0)}$
$H_1^{(0)}(t_{\times 1})$
$x_1(t_{\times 4})$
$x_1(t_{\times 1})$
$x_1$

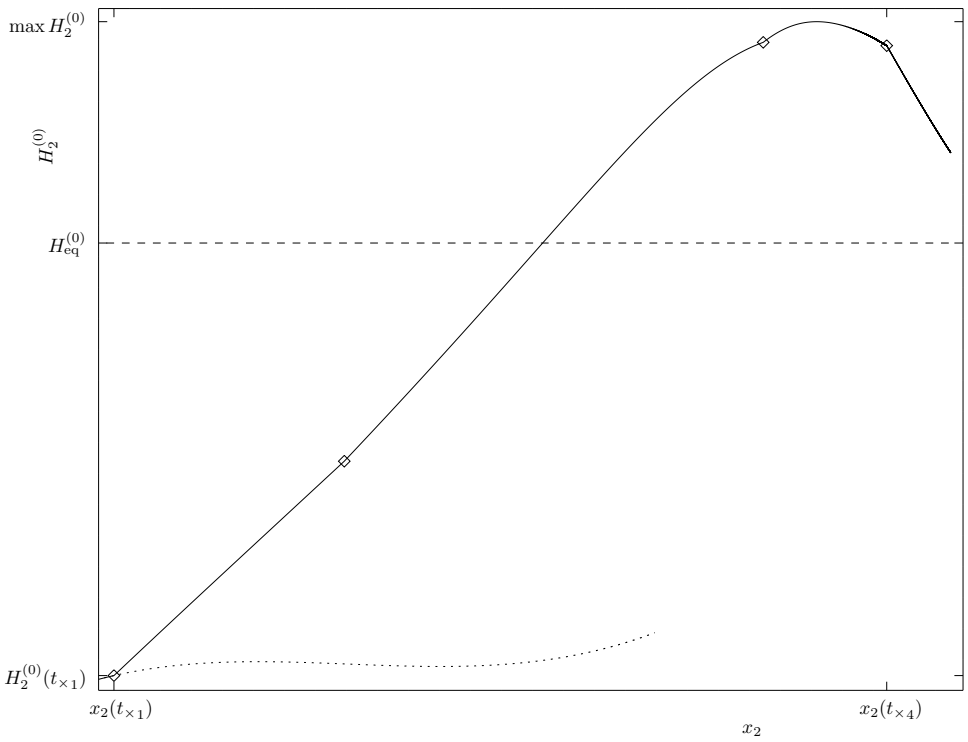


Figure 8: Trajectory parameterisation example for a triple of spikes and transition scenario of five intervals characterised by $\gamma = \left\{1, \frac{1}{4}, \frac{3}{20}, \frac{1}{10}, 1\right\}$ with cross-over moments $t_\times = \{1, 2, 6, 25\}$. Initial position is $\left(x_0, x_1, x_2\right) = \left(-\frac{3}{5}, \frac{1}{10}, \frac{3}{10}\right)$. Equilibrium position is $\left(x_0, x_1, x_2\right) = \left(-\frac{2}{3}, 0, \frac{2}{3}\right)$. Equilibrium height, equal for all spikes, is marked by the dashed line. Dotted lines show the trajectory for $\gamma \equiv 1$. Diamonds mark the cross-over moments $t_{\times j}$. Other parameters used: $(p, q, m, s) = (3, 2, 2, 0)$, $\epsilon = \frac{1}{10}$. Qualitatively similar results obtained with $(p, q, m, s) = (2, 1, 2, 0), (4, 2, 2, 0)$.

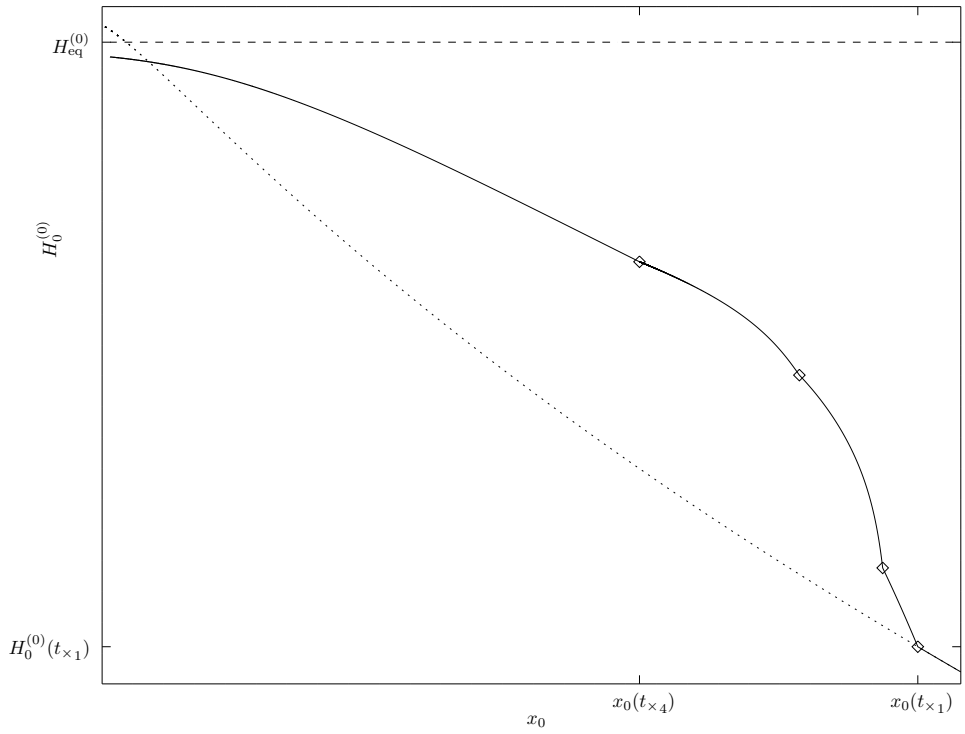
$H_{\rm eq}^{(0)}$
$H_0^{(0)}$
$H_0^{(0)}(t_{\times 1})$
$x_0(t_{\times 4})$
$x_0(t_{\times 1})$
$x_0$

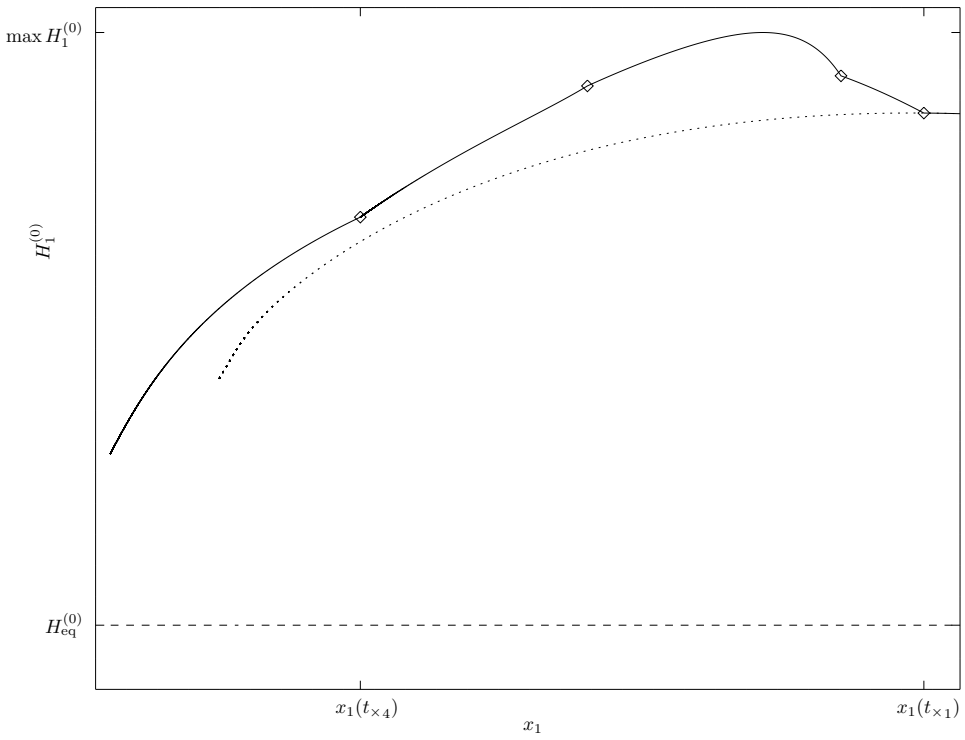
$\max H_1^{(0)}$
$H_1^{(0)}$
$H_{\rm eq}^{(0)}$
$x_1(t_{\times 4})$
$x_1(t_{\times 1})$
$x_1$

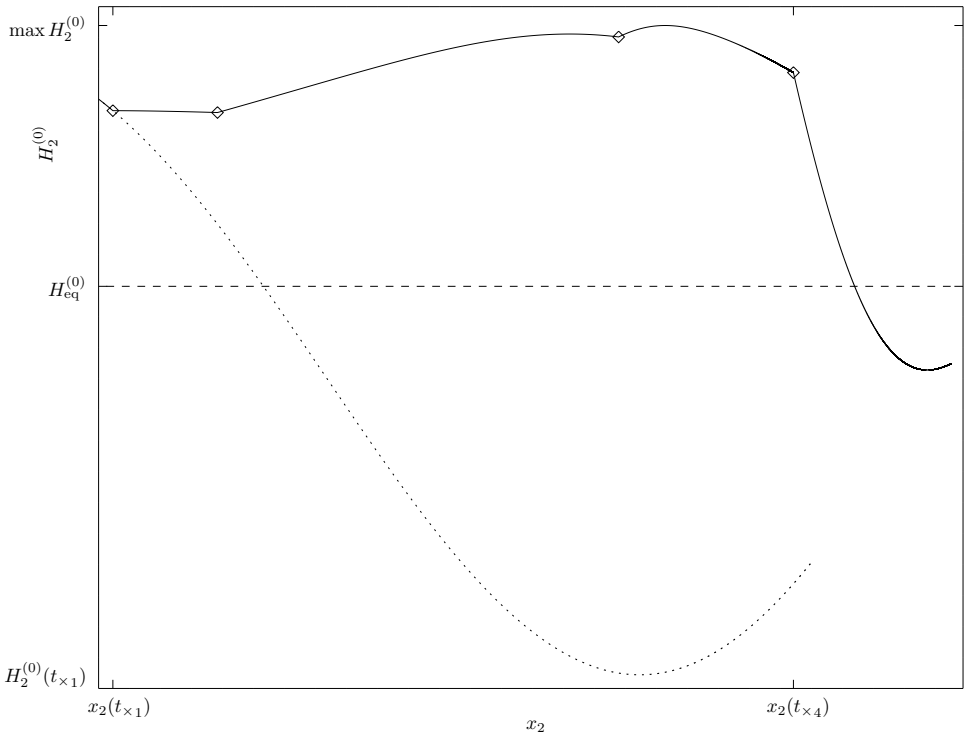


Figure 9: Trajectory parameterisation example for a triple of spikes and transition scenario of five intervals characterised by $\gamma = \left\{1, \frac{1}{4}, \frac{3}{20}, \frac{1}{10}, 1\right\}$ with cross-over moments $t_\times = \{1, 2, 6, 25\}$. Initial position is $\left(x_0, x_1, x_2\right) = \left(-\frac{3}{5}, \frac{1}{10}, \frac{3}{10}\right)$. Equilibrium position is $\left(x_0, x_1, x_2\right) = \left(-\frac{2}{3}, 0, \frac{2}{3}\right)$. Equilibrium height, equal for all spikes, is marked by the dashed line. Dotted lines show the trajectory for $\gamma \equiv 1$. Diamonds mark the cross-over moments $t_{\times j}$. Other parameters used: $(p, q, m, s) = (2, 1, 3, 0)$, $\epsilon = \frac{1}{10}$.

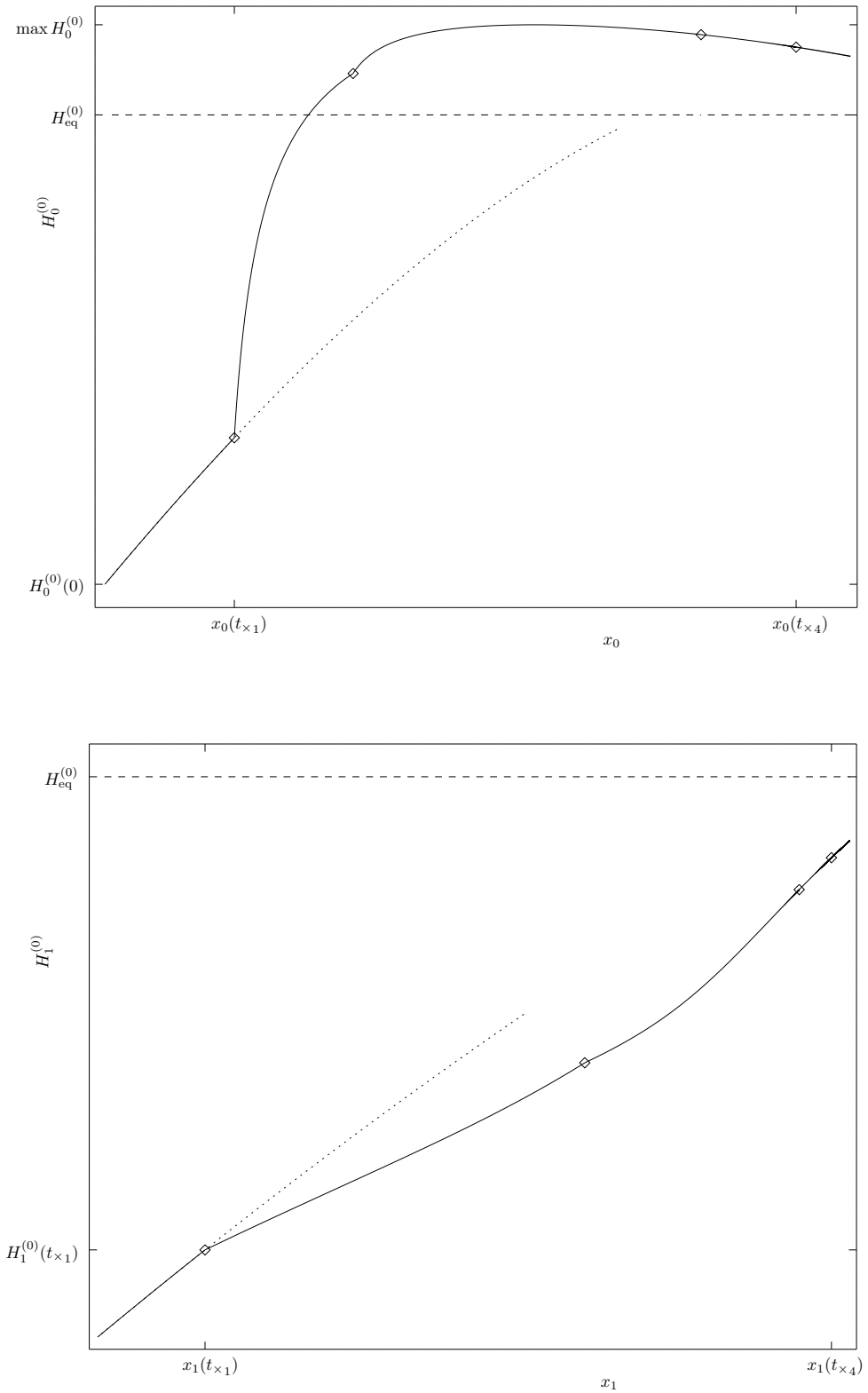


Figure 10: Trajectory parameterisation example for a symmetric quadruple of spikes and transition scenario of five intervals characterised by $\gamma = \left\{1, \frac{1}{4}, \frac{3}{20}, \frac{1}{10}, 1\right\}$ with cross-over moments $t_\times = \{8, 10, 20, 30\}$. Initial position is $\left(x_0, x_1\right) = \left(-\frac{19}{20}, -\frac{3}{4}\right)$. Equilibrium position is $\left(x_0, x_1\right) = \left(-\frac{3}{4}, -\frac{1}{4}\right)$. The two rightmost spikes satisfy $x_2(\tau) \equiv -x_1(\tau)$, $H_2^{(0)}(\tau) \equiv H_1^{(0)}(\tau)$, $x_3(\tau) \equiv -x_0(\tau)$, $H_3^{(0)}(\tau) \equiv H_0^{(0)}(\tau)$. Equilibrium height, equal for all spikes, is marked by the dashed line. Dotted lines show the trajectory for $\gamma \equiv 1$. Diamonds mark the cross-over moments $t_{\times j}$. Other parameters used: $(p, q, m, s) = (3, 2, 2, 0)$, $\epsilon = \frac{1}{10}$. Qualitatively similar results obtained with $(p, q, m, s) = (2, 1, 2, 0), (2, 1, 3, 0), (4, 2, 2, 0)$.

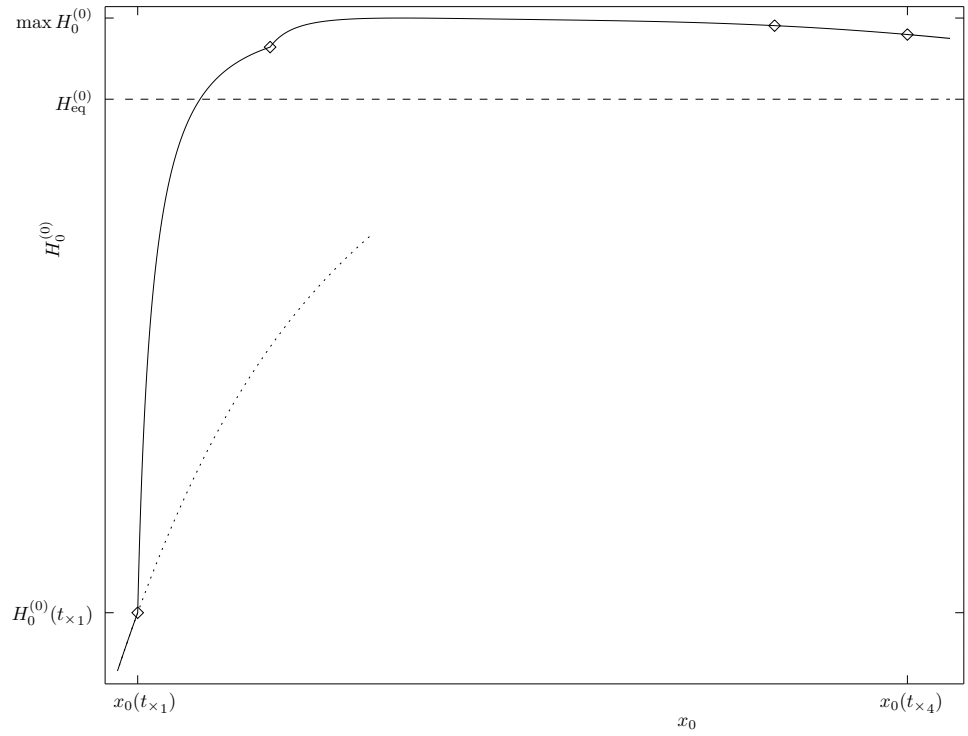
$\max H_0^{(0)}$
$H_{\mathrm{eq}}^{(0)}$
$H_0^{(0)}$
$H_0^{(0)}(t_{\times 1})$
$x_0(t_{\times 1})$
$x_0(t_{\times 4})$
$x_0$

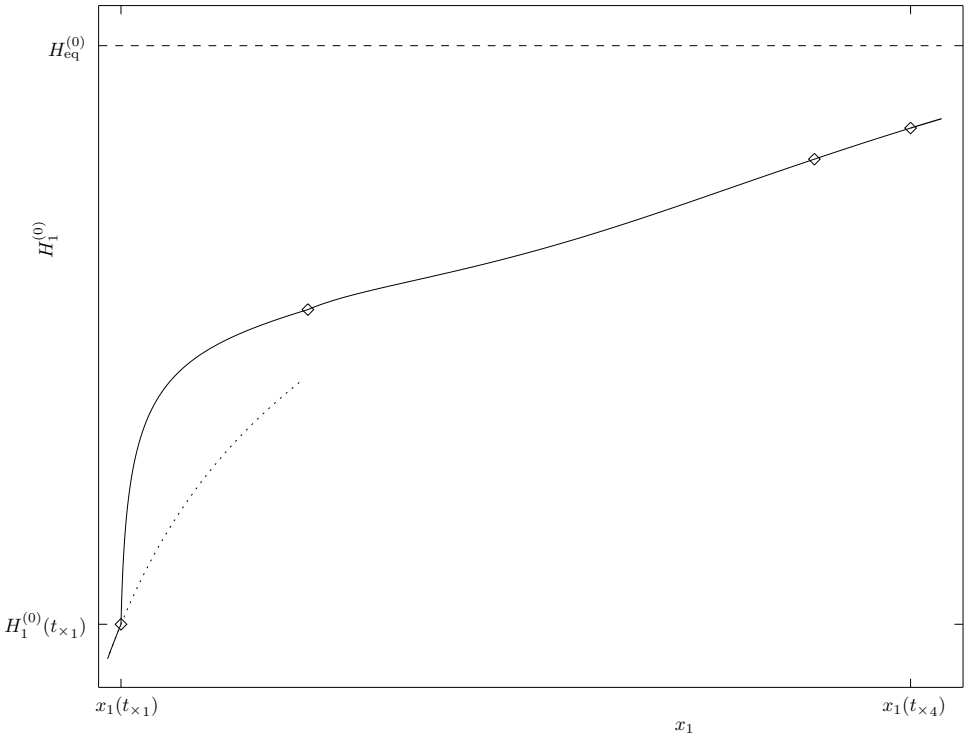
$H_{\mathrm{eq}}^{(0)}$
$H_1^{(0)}$
$H_1^{(0)}(t_{\times 1})$
$x_1(t_{\times 1})$
$x_1(t_{\times 4})$
$x_1$

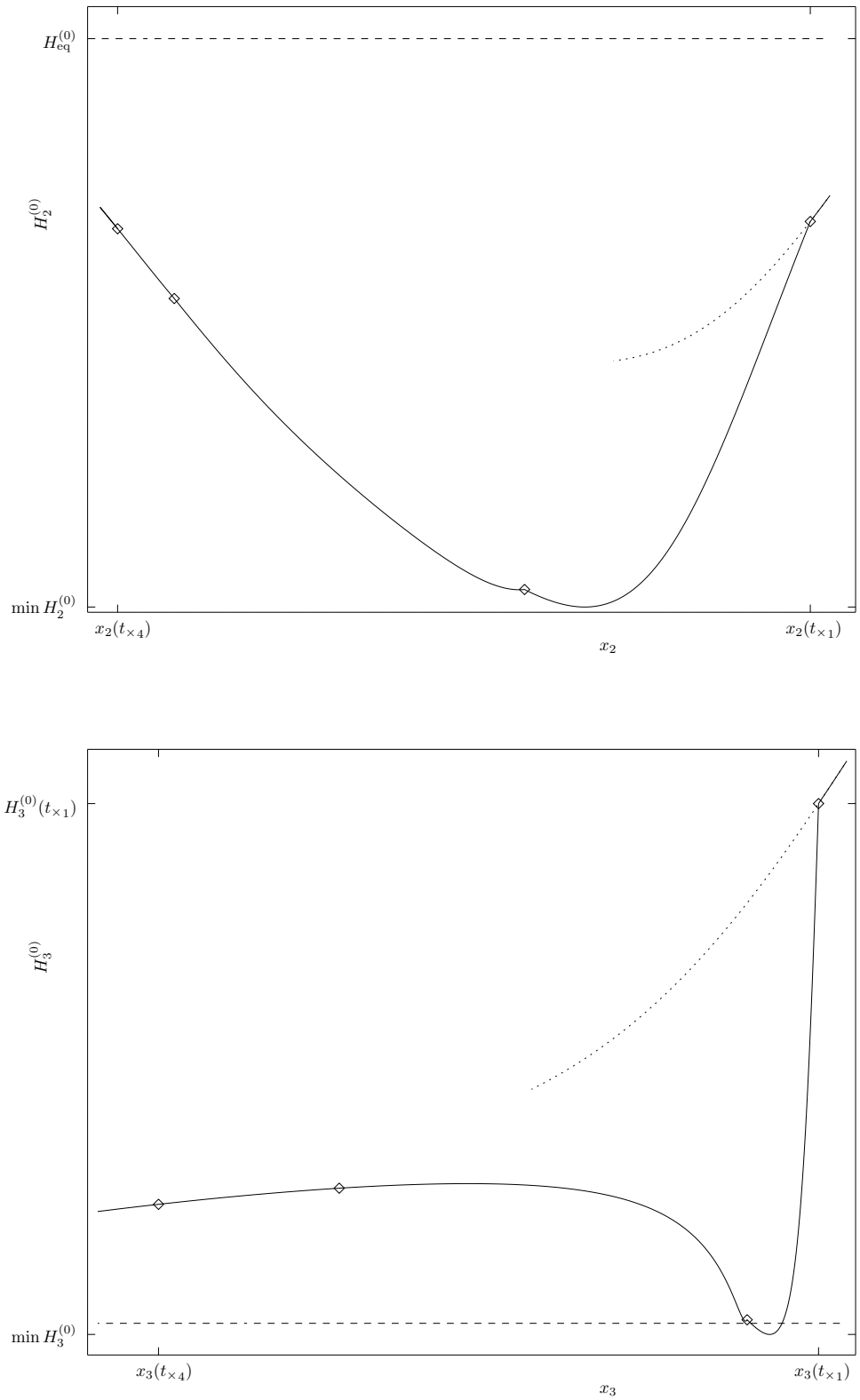


Figure 11: Trajectory parameterisation example for a quadruple of spikes and transition scenario of five intervals characterised by $\gamma = \left\{1, \frac{1}{4}, \frac{3}{20}, \frac{1}{10}, 1\right\}$ with cross-over moments $t_\times = \{1, 2, 6, 8\}$. Initial position is $\left(x_0, x_1, x_2, x_3\right) = \left(-\frac{19}{20}, -\frac{1}{2}, \frac{3}{5}, \frac{9}{10}\right)$. Equilibrium position is $\left(x_0, x_1, x_2, x_3\right) = \left(-\frac{3}{4}, -\frac{1}{4}, \frac{1}{4}, \frac{3}{4}\right)$. Equilibrium height, equal for all spikes, is marked by the dashed line. Dotted lines show the trajectory for $\gamma \equiv 1$. Diamonds mark the cross-over moments $t_{\times_j}$. Other parameters used: $(p, q, m, s) = (3, 2, 2, 0)$, $\epsilon = \frac{1}{10}$. Qualitatively similar results obtained with $(p, q, m, s) = (2, 1, 2, 0), (4, 2, 2, 0)$. With the set $(p, q, m, s) = (2, 1, 3, 0)$ the pattern failed to equilibrate.

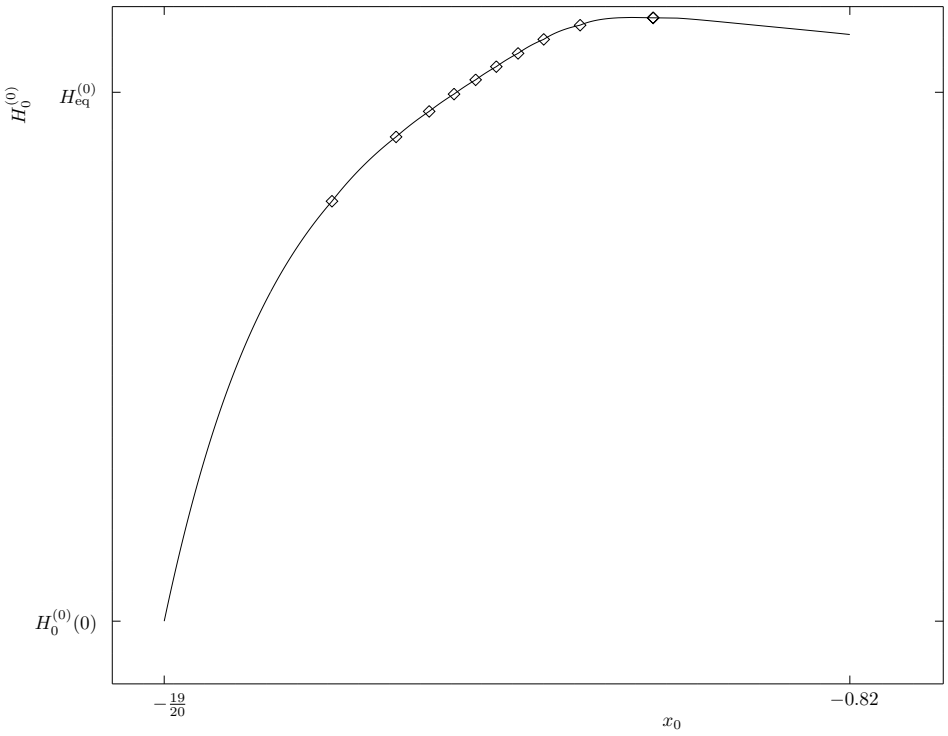
$H_0^{(0)}$
$H_{\mathrm{eq}}^{(0)}$
$H_0^{(0)}(0)$
$-\frac{19}{20}$
$-0.82$
$x_0$

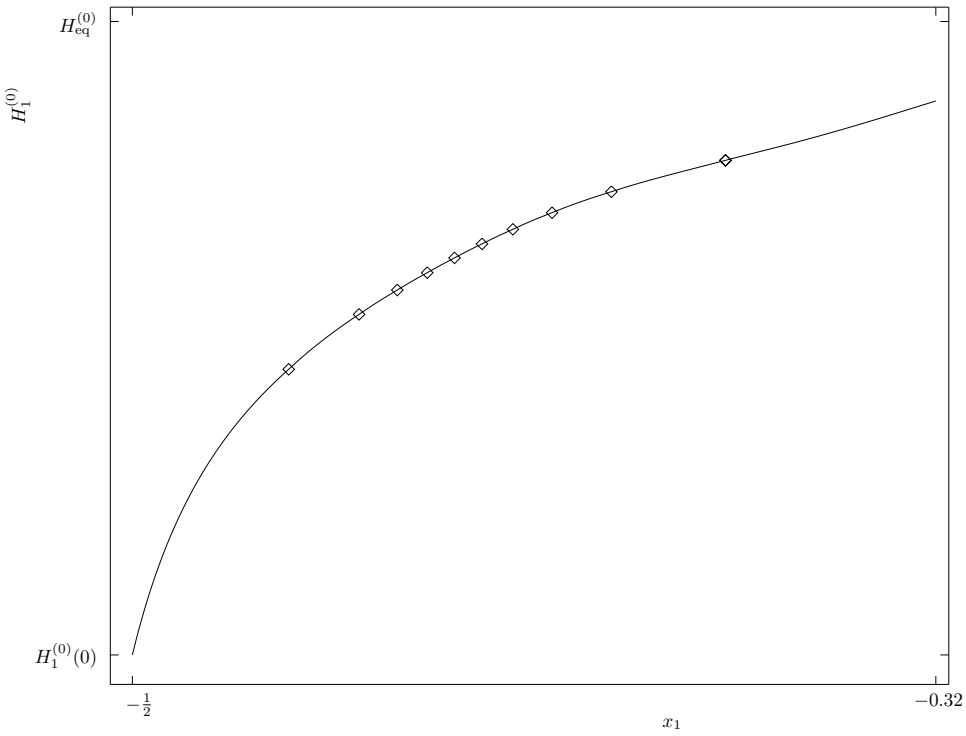
$H_1^{(0)}$
$H_{\mathrm{eq}}^{(0)}$
$H_1^{(0)}(0)$
$-\frac{1}{2}$
$-0.32$
$x_1$

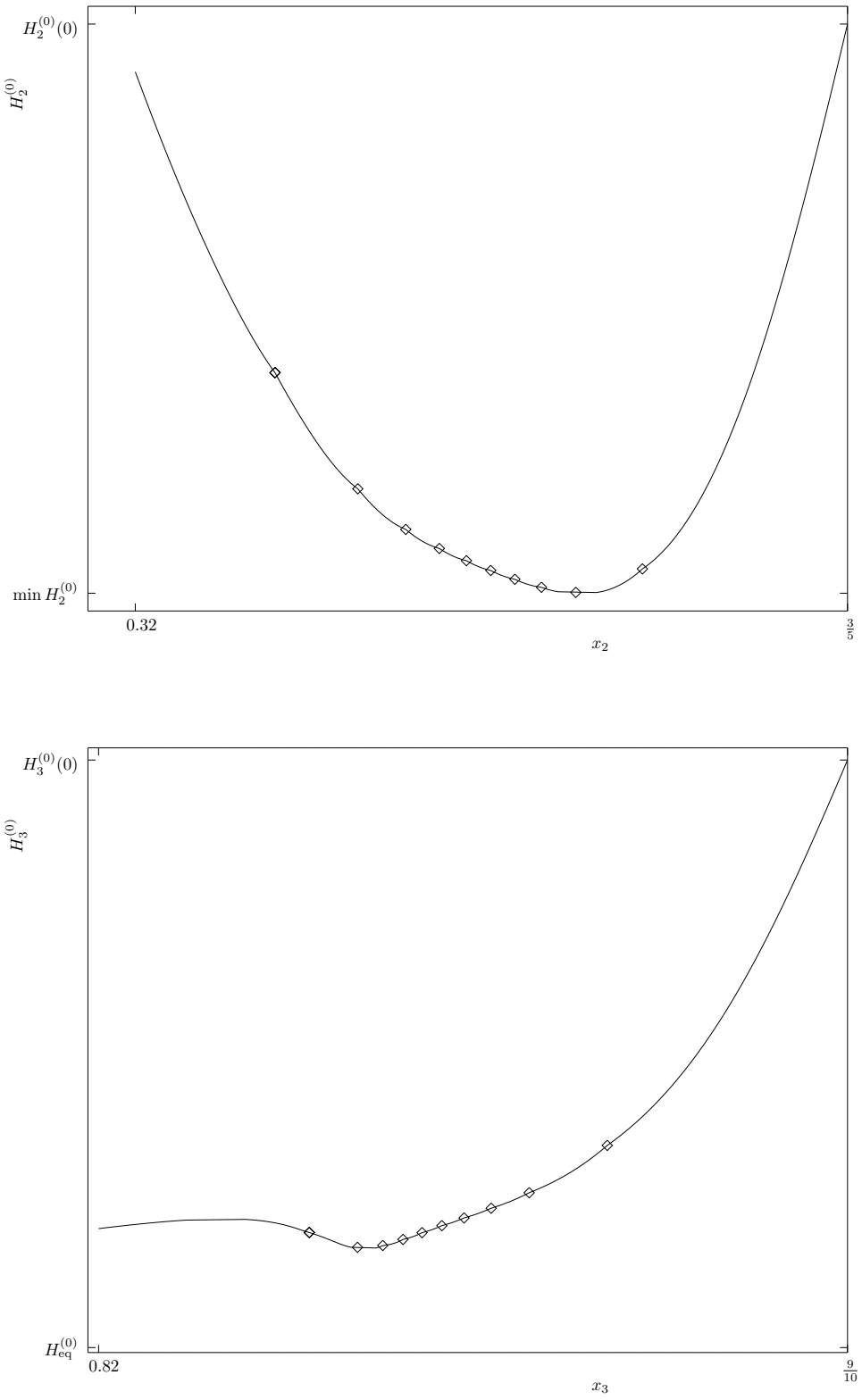


Figure 12: Trajectory parameterisation example for a quadruple of spikes and inner layer transition scenario (figure 1) with $\gamma_0 = \dfrac{3}{4}$, $\gamma_1 = \dfrac{3}{20}$ and $\varepsilon = 5$ in (6). Initial position is $\left(x_0, x_1, x_2, x_3\right) = \left(-\frac{19}{20}, -\frac{1}{2}, \frac{3}{5}, \frac{9}{10}\right)$. Equilibrium position is $\left(x_0, x_1, x_2, x_3\right) = \left(-\frac{3}{4}, -\frac{1}{4}, \frac{1}{4}, \frac{3}{4}\right)$. Diamonds mark the cross-over moments $t_{\times_j}$. Other parameters used: $(p, q, m, s) = (3, 2, 2, 0)$, $\epsilon = \frac{1}{10}$. Qualitatively similar results obtained with $(p, q, m, s) = (2, 1, 2, 0), (4, 2, 2, 0)$.

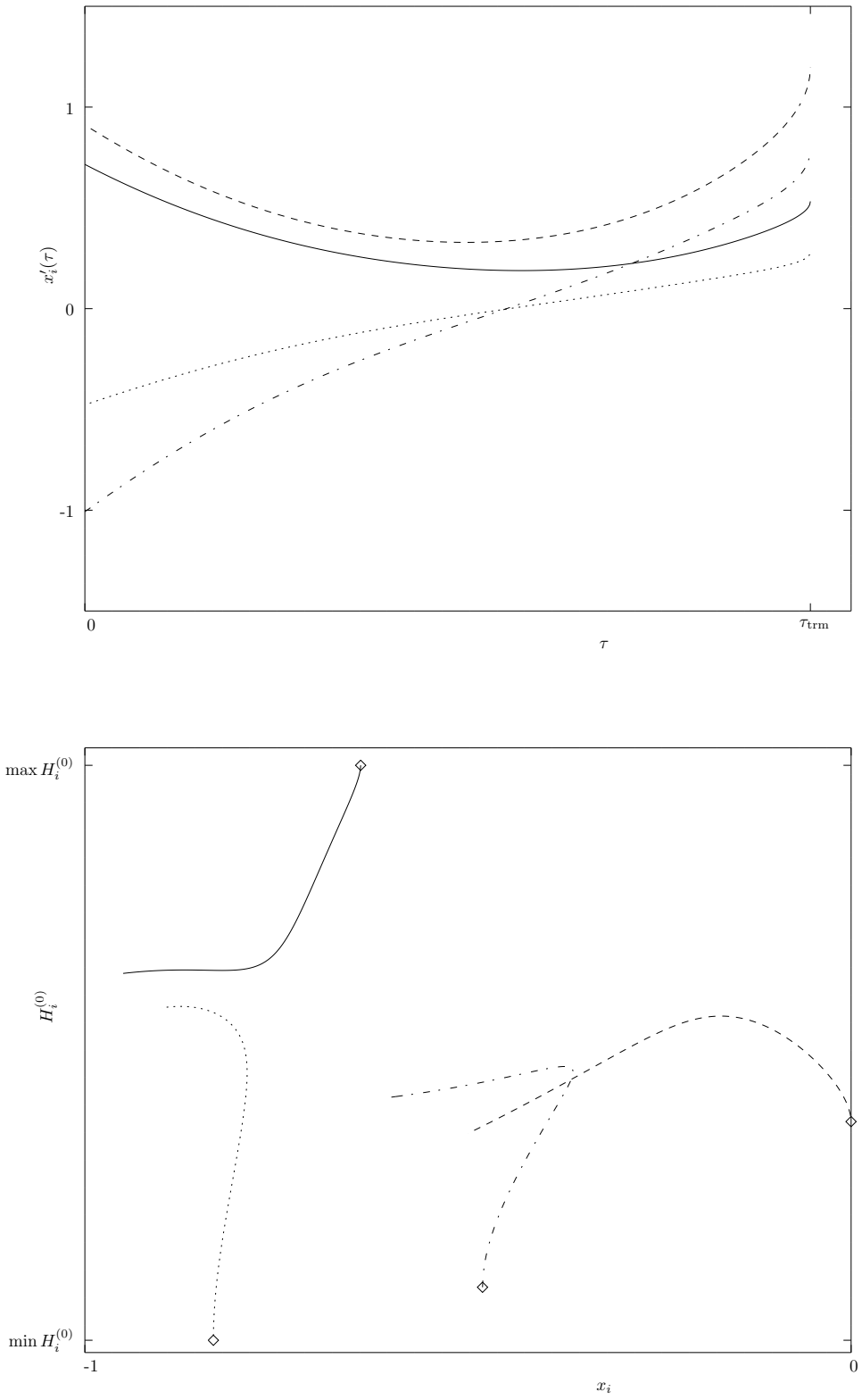


Figure 13: Example of trajectory termination due to a bifurcation for a quadruple of spikes with $\gamma \equiv 1$. Top panel: velocity $x_i'(\tau)$, $i = 0$ (leftmost spike, solid curve), $i = 1$ (left central spike, dashed curve), $i = 2$ (right central spike, dash-dotted curve) and $i = 3$ (rightmost spike, dotted curve). Bottom panel: $H_i^{(0)}(x_i)$ for the left spikes, $i = \{0, 1\}$, and $H_i^{(0)}(-x_i)$ for the right ones, $i = \{2, 3\}$. Diamonds mark trajectory termini. Curve line styles are identical to top panel. Initial position is $\Big(x_0, x_1, x_2, x_3\Big) = \Big(-\frac{19}{20}, -\frac{1}{2}, \frac{3}{5}, \frac{9}{10}\Big)$. Equilibrium position $\Big(x_0, x_1, x_2, x_3\Big) = \Big(-\frac{3}{4}, -\frac{1}{4}, \frac{1}{4}, \frac{3}{4}\Big)$ is never reached, the terminus point $\tau_{\rm trm}$ characterised by infinite slope of $x_i'(\tau)$. Other parameters used: $(p, q, m, s) = (3, 3, 3, 0)$, $\epsilon = \frac{1}{10}$.

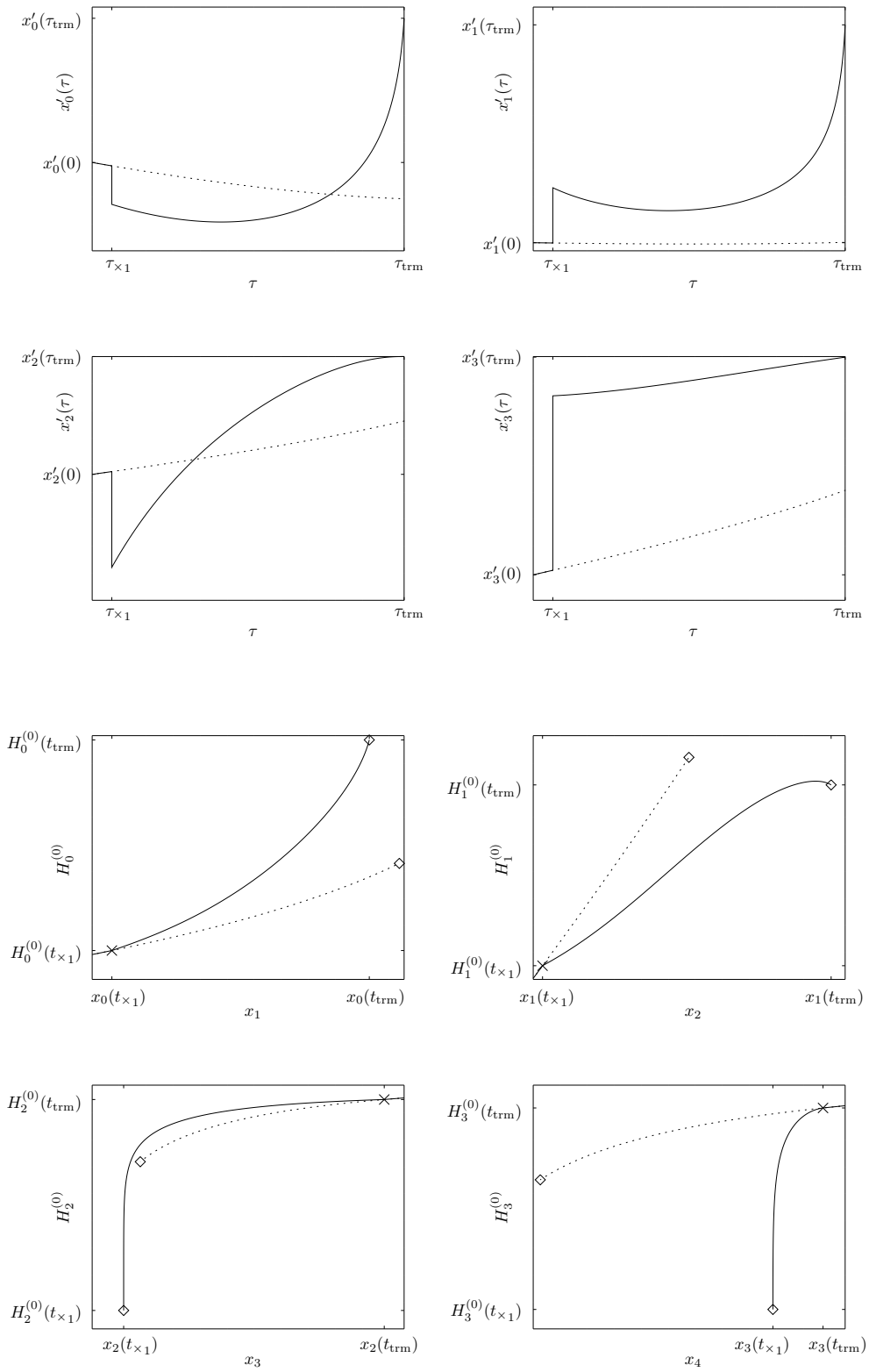


Figure 14: Example of trajectory termination due to a bifurcation for a quadruple of spikes with $\gamma = \left\{1, \frac{1}{4}\right\}$ and cross-over moment $t_\times = 1$. Top: velocity $x_i'(\tau)$. Solid curves: $i = 0$ (leftmost spike), $i = 1$ (left central spike), $i = 2$ (right central spike) and $i = 3$ (rightmost spike). Dotted curves show the same evolution for $\gamma \equiv 1$. Bottom: respective $H_i^{(0)}(x_i)$. Diamonds mark trajectory termini. Crosses mark the cross-over moment. Initial position is $\Big(x_0, x_1, x_2, x_3\Big) = \Big(-\frac{19}{20}, -\frac{1}{2}, \frac{3}{5}, \frac{9}{10}\Big)$. Equilibrium position $\Big(x_0, x_1, x_2, x_3\Big) = \Big(-\frac{3}{4}, -\frac{1}{4}, \frac{1}{4}, \frac{3}{4}\Big)$ is never reached, the terminus point $\tau_{\rm trm}$ characterised by infinite slope of $x_i'(\tau)$ for the the left pair of spikes, $x_i'(\tau_{\rm trm}) = 0$ for the right pair. Other parameters used: $(p, q, m, s) = (2, 1, 3, 0)$, $\epsilon = \frac{1}{10}$.